Eur. Phys. J. B **25**, 445–462 (2002)
DOI: 10.1140/epjb/e20020051

THE EUROPEAN PHYSICAL JOURNAL B
EDP Sciences

T-matrix analysis of biexcitonic correlations in the nonlinear optical response of semiconductor quantum wells

R. Takayama[1,a], N.H. Kwong[1], I. Rumyantsev[2], M. Kuwata-Gonokami[3], and R. Binder[2]

[1] Cooperative Excitation Project, ERATO, Japan Science and Technology Corporation, Optical Sciences Center, University of Arizona, Tucson, AZ 85721, USA
[2] Optical Sciences Center, University of Arizona, Tucson, AZ 85721, USA
[3] Cooperative Excitation Project, ERATO, Japan Science and Technology Corporation, Department of Applied Physics, University of Tokyo, 7-3-1 Hongo, Bunkyo-ku, Tokyo 113-8656, Japan

Received 3 August 2001 and Received in final form 26 December 2001

Abstract. A detailed numerical analysis of exciton-exciton interactions in semiconductor quantum wells is presented. The theory is based on the dynamics-controlled truncation formalism and evaluated for the case of resonant excitation of 1s-heavy-hole excitons. It is formulated in terms of standard concepts of scattering theory, such as the forward-scattering amplitude (or T-matrix). The numerical diagonalization of the exciton-exciton interaction matrix in the 1s-approximation yields the excitonic T-matrix. We discuss the role of the direct and exchange interaction in the effective two-exciton Hamiltonian, which determines the T-matrix, evaluated within the 1s-subspace, and also analyze the effects of the excitonic wave function overlap matrix. Inclusion of the latter is shown to effectively prevent the 1s-approximation from making the Hamiltonian non-hermitian, but a critical discussion shows that other artefacts may be avoided by not including the overlap matrix. We also present a detailed analysis of the correspondence between the excitonic T-matrix in the 1s-approximation and the well-known T-matrix governing two-particle interactions in two dimensional systems *via* short-range potentials.

PACS. 78.67.De Quantum wells – 03.65.Nk Scattering theory – 71.35.Gg Exciton-mediated interactions

1 Introduction

Nonlinear semiconductor optics offers the unique possibility to study many-body processes and particle correlations in almost arbitrary geometries and spatial dimensions. Probably the best-studied case is that of quasi-two-dimensional systems, which is realized in the form of semiconductor quantum wells. The theoretical analysis of many-body effects in semiconductor quantum wells can roughly be divided into two limiting cases, that of high electron-hole excitation on the one hand and, on the other hand, that of low excitation, specifically in the lowest-order nonlinear optical regime ($\chi^{(3)}$-regime). Coherent optical experiments and corresponding theoretical investigations have clearly shown that the third-order nonlinear regime yields important information about quantum correlations, exciton-scattering and the formation of coherent biexcitons (see, for example, [1–26]; further references can be found in [27]). Many of the theoretical $\chi^{(3)}$-studies are based on the dynamics-controlled truncation (DCT) scheme [28]. It has proven to be a powerful approach to two-exciton correlations (see, for example, [8,10,19,26,29,30]). However, owing to the complicated dependence of the measured signals on the exciton scattering amplitude, the question how these many-body effects are related to standard concepts in scattering theory (see, *e.g.*, [31]) is usually not addressed. Clearly, the identification of theoretical concepts in coherent exciton correlations with old and well-established concepts in standard scattering theory would deepen our understanding of excitonic optical nonlinearities. It can also make contributions to standard scattering theory since exciton-scattering can be realized experimentally in otherwise not easily accessible geometries (here: quasi-two-dimensional systems).

An important concept in standard scattering theory is that of the T-matrix or scattering amplitude, which also plays a prominent role in conventional equilibrium and nonequilibrium many-body theory. Specifically, the 'off-energy-shell' (for a definition, see Sect. 2 below) forward scattering amplitude between two constituent particles governs the statistical mechanical properties of a dilute non-ideal quantum gas (see, *e.g.*, [32–34]) and is also important in dense quantum systems (see, *e.g.*, [35]). The 'on-energy-shell' T-matrix controls the collisional relaxation rate of a gas in a Boltzmann kinetic description.

While it might be intuitively clear that exciton-exciton scattering should somehow be describable in terms of the

[a] e-mail: takayama@u.arizona.edu

concepts and language developed in the field of standard two-body scattering theory, it turns out that the correspondences and analogies are quite complicated, and that they require a detailed analysis which states the exact conditions for those correspondences and analogies to hold. It is the goal of this paper to present such an analysis for the specific case of $\chi^{(3)}$ response dominated by 1s-heavy-hole excitons. This is probably the best-studied case and it allows, in our opinion, the closest conceptual link between nonlinear semiconductor optics and standard scattering theory. The underlying reason for this link to be valid only in an approximate fashion is the fact that excitons are inherently composite particles (for which the simplest scattering process involves four particles, two electrons and two holes). One consequence of the exciton's compositeness is the fact that the interaction matrix elements consist of direct and exchange contributions. Also, in higher-order scattering processes the intermediate states can be excitons with higher internal quantum numbers (apart from 1s-excitons with arbitrary of center-of-mass momentum). Yet another consequence is that the asymptotic states for a scattering event – product two-exciton plane wave states antisymmetrized with respect to the electron pair and the hole pair – are not exactly orthonormal to each other.

Although the situation here bears some similarity to the collision between two hydrogen atoms studied in depth in atomic physics, there are two crucial differences. First, coherent excitons are created (by the external field) with an energy-momentum relation closer to that of photons than that of real free excitons, while in an atomic collision experiment, real free atoms are prepared in the initial state and measured in the final state. One consequence, among others, of this difference is that coherent (virtual) excitons can be created with the right energies and momenta for them to scatter into a bound biexciton, while the hydrogen molecule is ruled out by energy conservation as a physical final state in a collision between two (real) hydrogen atoms. In scattering language, the two types of experiments probe two different parts of the T-matrix. The second difference is that the electron-hole mass ratios in semiconductors are generally much larger than the electron-proton mass ratio which is practically zero. It turns out that the T-matrix, and the complications arising from the exciton's fermion constituents, have a non-trivial dependence on the electron-hole mass ratio.

Apart from all these aspects, which will be addressed in detail in this paper, we are also interested in identifying exact analogies between the exciton-T-matrix and conventional T-matrices in two dimensions for two-particle scattering with (generic) short-range potentials. The fact that we are dealing with a quasi-two-dimensional system is important in the sense that, in 2D, the ordinary T-matrix follows some generic (independent of the potential) low-energy behaviors which are distinctive of the system's dimensionality only ([33]). It is interesting to see if the exciton-T-matrix exhibits the same behaviors. All of the above issues, which will be examined below, are intimately related to the question: to what extent can one express the theory of $\chi^{(3)}$ optical response of a quantum well as an effective theory of interacting 'elementary' excitons?

In the following section, we review the DCT formalism and give detailed account of our approach. In Section 3 we present a detailed discussion of the excitonic T-matrix based on our numerical results. This includes a discussion of contributions from other than 1s-exciton states, details of the excitonic interaction potential, the role of the exciton wave function overlap matrix, the biexciton binding energy, and the properties of the off-energy-shell T-matrix. In Section 4 we summarize the work presented in this paper.

2 Theory

In this section we review the basic set of equations of the DCT theory [28], evaluated in third-order in the light field amplitude.

As for the measurement configuration, we assume to have a single quantum well and one or two incoming light pulses. The pulses are assumed to propagate normal to the quantum well (QW). However, in the case of two light pulses we assume the two propagation directions to be slightly different, so that the pulses (called pump and/or probe) can be distinguished by their direction, while the selection rules for both are assumed to be those for normal incidence.

2.1 $\chi^{(3)}$ dynamics controlled truncation equations in the exciton basis

We start with the Hamiltonian of the many-particle system in two dimensions coupled to an external electromagnetic field,

$$H = H_1 + H_2 + H_{\text{field}}, \tag{1}$$

$$H_1 = \sum_{\mathbf{k}s} E_s(\mathbf{k}) a_s^\dagger(\mathbf{k}) a_s(\mathbf{k}) + \sum_{\mathbf{k}j} E_j(\mathbf{k}) a_j^\dagger(\mathbf{k}) a_j(\mathbf{k}), \tag{2}$$

$$\begin{aligned} H_2 = \frac{1}{2A} \sum_{\mathbf{q}\neq 0,\mathbf{k},\mathbf{k}'} V(\mathbf{q}) \\ \times \Bigg[\sum_{ss'} a_s^\dagger(\mathbf{k}+\mathbf{q}) a_{s'}^\dagger(\mathbf{k}'-\mathbf{q}) a_{s'}(\mathbf{k}') a_s(\mathbf{k}) \\ + \sum_{jj'} a_j^\dagger(\mathbf{k}+\mathbf{q}) a_{j'}^\dagger(\mathbf{k}'-\mathbf{q}) a_{j'}(\mathbf{k}') a_j(\mathbf{k}) \\ - \sum_{sj} \Big(a_s^\dagger(\mathbf{k}+\mathbf{q}) a_j^\dagger(\mathbf{k}'-\mathbf{q}) a_j(\mathbf{k}') a_s(\mathbf{k}) \\ + a_j^\dagger(\mathbf{k}+\mathbf{q}) a_s^\dagger(\mathbf{k}'-\mathbf{q}) a_s(\mathbf{k}') a_j(\mathbf{k}) \Big) \Bigg], \end{aligned} \tag{3}$$

$$H_{\text{field}} = \sum_{sj\mathbf{k}} \Big[\mathbf{d}_{sj} \cdot \mathbf{E}(t) a_s^\dagger(\mathbf{k}) a_j(-\mathbf{k}) + \mathbf{d}_{js} \cdot \mathbf{E}(t) a_j^\dagger(-\mathbf{k}) a_s(\mathbf{k}) \Big] \tag{4}$$

where s denotes the set of quantum numbers (band index, spin projection) other than two-dimensional momentum assigned to a single electron orbital in a conduction

band, and j denotes the set for a hole orbital in a valence band. $E_s(E_j)$ is the band-model single electron (hole) energy, $\mathbf{d}_{sj} \equiv q_{\rm e}\langle s|\mathbf{r}|j\rangle$ is the transition dipole matrix element, $V(\mathbf{q}) = \frac{2\pi {q_{\rm e}}^2}{\epsilon_b|\mathbf{q}|}$, $q_{\rm e}$ is the magnitude of the electron's charge, ϵ_b is the background dielectric constant of the QW material, and A is the area of the normalization box. For simplicity, the single-particle part H_1 is assumed to be diagonal in the band indices. Only the part of the Coulomb interaction that does not cause an interband transition is retained in the model. This approximation makes the tremendous simplification of the many-body problem in the DCT formalism possible. The ground state of the system is the electron-hole vacuum, which is assumed to be stable against electron-hole creation by virtue of a large enough band gap.

The dynamics controlled truncation (DCT) scheme [28] provides a formalism for studying Coulomb correlations in weakly-nonlinear coherent optics of semiconductors. Under the assumptions that (i) the initial state is the ground state, and (ii) the Coulomb interaction does not induce interband transitions, DCT systematically and rigorously truncates, at each order of the applied field, the infinite hierarchy of coupled equations of motion of density matrices. To each perturbation (in the applied field) order, all Coulomb correlations are exactly carried by the resulting closed equations. In this paper, the third order DCT equation will be used to relate measurable quantities in the coherent nonlinear regime to the common concept of two-dimensional scattering (between excitons). The DCT equations govern the evolution of *fermionic* density matrices. To have a description based on excitons, we will follow [36–38] in transforming the equations from the electron-hole basis to the exciton basis.

In $\chi^{(3)}$, only two density matrices, the interband polarization and the coherent biexcitonic amplitude, need to be considered. The interband polarization in the exciton basis is defined as:

$$p_n^{sj}(t) = \sum_{\mathbf{k}} \phi_n^{sj*}(\mathbf{k})\langle a_j(-\mathbf{k},t)a_s(\mathbf{k},t)\rangle, \tag{5}$$

where $\phi_n^{sj}(\mathbf{k})$ is the nth lowest exciton eigenfunction consisting of an electron from band s and a hole from band j, $\langle\cdots\rangle$ denotes averaging with respect to the initial density operator, and the creation (annihilation) operators are in the Heisenberg representation. In general, the interband polarization also depends on the momentum $\mathbf{q}$ governing the center-of-mass motion, but in our Hamiltonian equation (1), we have assumed that the excitation is spatially homogeneous, allowing only for an interband polarization with $\mathbf{q} = 0$. The coherent biexcitonic amplitude in the 2D single-particle momentum basis is defined as:

$$\begin{aligned} b_{sjs'j'}(\mathbf{k}_1,\mathbf{k}_2,\mathbf{k}_3,\mathbf{k}_4,t) = \\ &\left\langle a_{j'}(-\mathbf{k}_4,t)a_{s'}(\mathbf{k}_3,t)a_j(-\mathbf{k}_2,t)a_s(\mathbf{k}_1,t)\right\rangle \\ &- \left\langle a_{j'}(-\mathbf{k}_4,t)a_{s'}(\mathbf{k}_3,t)\right\rangle\left\langle a_j(-\mathbf{k}_2,t)a_s(\mathbf{k}_1,t)\right\rangle \\ &+ \left\langle a_{j'}(-\mathbf{k}_4,t)a_s(\mathbf{k}_1,t)\right\rangle\left\langle a_j(-\mathbf{k}_2,t)a_{s'}(\mathbf{k}_3,t)\right\rangle . \end{aligned} \tag{6}$$

For spatially homogeneous excitations, we have the condition $\mathbf{k}_1-\mathbf{k}_2+\mathbf{k}_3-\mathbf{k}_4 = \mathbf{0}$. We specialize to the case where only one conduction band is involved so that s denotes only the spin projection along the normal to the QW's plane. This electron spin is taken to be $s = \pm 1/2$. The exciton wavefunctions are assumed to be independent of the electron spin, which is then dropped from the wavefunction symbol. Moreover, since the interactions among the four fermions are spin-independent, the $(2e, 2h)$ Hamiltonian is block diagonal in the eigenstates of the total electron spin. It is therefore advantageous to use linear combinations of $b_{sjs'j'}$ that correspond to these eigenstates:

$$\begin{aligned} b^{\lambda}_{sjs'j'}(\mathbf{k}_1,\mathbf{k}_2,\mathbf{k}_3,\mathbf{k}_4,t) = \frac{1}{2}\,[&b_{sjs'j'}(\mathbf{k}_1,\mathbf{k}_2,\mathbf{k}_3,\mathbf{k}_4,t) \\ &+\lambda b_{s'jsj'}(\mathbf{k}_1,\mathbf{k}_2,\mathbf{k}_3,\mathbf{k}_4,t)]\,, \end{aligned} \tag{7}$$

where $\lambda = +1(-1)$ labels the channel with total electron spin 1(0) or triplet(singlet). Taking the effective mass approximation for the electrons and the holes, we can also expand $b^{\lambda}_{sjs'j'}$ in a two-exciton basis:

$$\begin{aligned} &b^{\lambda}_{sjs'j'}(\mathbf{k}_1,\mathbf{k}_2,\mathbf{k}_3,\mathbf{k}_4) = \\ &\sum_{nm}\Big[\phi_n^{j}(\alpha\mathbf{k}_1+\beta\mathbf{k}_2)\phi_m^{j'}(\alpha'\mathbf{k}_3+\beta'\mathbf{k}_4)b_{nm}^{sjs'j'\lambda}(\mathbf{k}_1-\mathbf{k}_2) \\ &\quad -\lambda\,\phi_n^{j}(\alpha\mathbf{k}_3+\beta\mathbf{k}_2)\phi_m^{j'}(\alpha'\mathbf{k}_1+\beta'\mathbf{k}_4)b_{nm}^{sjs'j'\lambda}(\mathbf{k}_3-\mathbf{k}_2)\Big] \end{aligned} \tag{8}$$

where $\alpha = m_j/M_j$ and $\beta = m_{\rm e}/M_j$ are the ratios of the hole (m_j) mass, which depends on the band j, and the electron ($m_{\rm e}$) mass to the exciton mass $M_j = m_{\rm e} + m_j$, and α' and β' are similarly related to $m_{j'}$. This expansion, borrowed from molecular physics, has the advantage over an expansion using only the first (direct) term that the (anti)symmetry of $b^{\lambda}_{sjs'j'}(\mathbf{k}_1,\mathbf{k}_2,\mathbf{k}_3,\mathbf{k}_4)$ in the four-fermion momentum space is satisfied for each combination of (n, m) (antisymmetry under electron exchange imposes no restrictions on the expansion coefficient $b_{nm}^{sjs'j'\lambda}(\mathbf{q})$, while antisymmetry under hole exchange imposes the condition $b_{mn}^{sj's'j\lambda}(-\mathbf{q}) = b_{nm}^{sjs'j'\lambda}(\mathbf{q})$). In other words, proper exchange antisymmetry of the four-fermion system would be retained in the theory under any truncation of the exciton basis. The coefficients, representing the coherent biexcitonic correlation function for two excitons with center-of-mass momenta $\mathbf{q}$ and $-\mathbf{q}$, internal quantum numbers n and m, and involving two electrons in bands s and s' and two holes in bands j and j', are given by

$$\begin{aligned} b_{nm}^{sjs'j'\lambda}(\mathbf{q}) = &\sum_{n'm'\mathbf{q}'}\left(1-\lambda S^{jj'}\right)^{-1}_{nmn'm'}(\mathbf{q},\mathbf{q}')\sum_{\mathbf{k}\mathbf{k}'}\phi_{n'}^{j*}(\mathbf{k}+\alpha\mathbf{q}') \\ &\phi_{m'}^{j'*}(\mathbf{k}'+\beta'\mathbf{q}')\,b^{\lambda}_{sjs'j'}(\mathbf{k}+\mathbf{q}',\mathbf{k},\mathbf{k}',\mathbf{k}'+\mathbf{q}'). \end{aligned} \tag{9}$$

The presence of the overlap matrix

$$\begin{aligned} S^{jj'}_{nmn'm'}(\mathbf{q},\mathbf{q}') = \sum_{\mathbf{k}}\phi_n^{j*}(\mathbf{k}+\alpha\mathbf{q})\,\phi_m^{j'*}(\mathbf{k}+\mathbf{q}'+\beta'\mathbf{q}) \\ \times\,\phi_{n'}^{j}(\mathbf{k}+\alpha\mathbf{q}')\,\phi_{m'}^{j'}(\mathbf{k}+\mathbf{q}+\beta'\mathbf{q}')\,, \end{aligned} \tag{10}$$

expresses the antisymmetry of $b^{\lambda}_{sjs'j'}(\mathbf{k}_1,\mathbf{k}_2,\mathbf{k}_3,\mathbf{k}_4)$, or equivalently, the fact that the basis of antisymmetrized two-exciton states is not orthogonal. In equation (9), $S^{jj'}_{nmn'm'}(\mathbf{q},\mathbf{q}')$ should be seen as a matrix in the basis labeled by the set $(n,m,\mathbf{q})$, with j,j' being parameters. It is in this way that the inverse matrix $(1-\lambda S^{jj'})^{-1}$ is defined.

Transforming the $\chi^{(3)}$-DCT equations from the electron-hole momentum basis to the exciton basis [38], one gets a closed, coupled set of equations of motion for $p^{sj}_n(t)$ and $b^{sjs'j'\lambda}_{nm}(\mathbf{q},t)$:

$$\begin{aligned}\mathrm{i}\hbar\frac{\mathrm{d}}{\mathrm{d}t}p^{sj}_n &= \left(\varepsilon^{sj}_n(0)-\mathrm{i}\gamma_2\right)p^{sj}_n - \Omega_{sj}\tilde{\phi}^{j*}_n(\mathbf{0})\\ &+\sum_{s'j'mm'}\left[\Omega_{s'j}A^{jj'j'}_{nmm'}p^{sj'}_{m'}p^{s'j'*}_{m}+\Omega_{sj'}A^{jj'j}_{nmm'}p^{s'j}_{m'}p^{s'j'*}_{m}\right]\\ &+\sum_{s'j'mn'm'}V^{\mathrm{HF}(jj')}_{nmn'm'}p^{s'j}_{n'}p^{sj'}_{m'}p^{s'j'*}_{m}\\ &+\sum_{s'j'mn'm'\lambda\mathbf{q}'}p^{s'j'*}_{m}W^{xx(jj'\lambda)*}_{n'm'nm}(\mathbf{q},\mathbf{0})b^{sjs'j'\lambda}_{n'm'}(\mathbf{q}) \quad (11)\end{aligned}$$

$$\begin{aligned}\mathrm{i}\hbar\frac{\mathrm{d}}{\mathrm{d}t}b^{sjs'j'\lambda}_{nm}(\mathbf{q}) &= \sum_{n'm'\mathbf{q}'}H^{xx(jj'\lambda)}_{nmn'm'}(\mathbf{q},\mathbf{q}')\,b^{sjs'j'\lambda}_{n'm'}(\mathbf{q}')\\ &-\mathrm{i}\gamma_b b^{sjs'j'\lambda}_{nm}(\mathbf{q})+\sum_{n'm'rs\mathbf{q}'}\frac{1}{2}\Big(1-\lambda S^{jj'}\Big)^{-1}_{nmrs}(\mathbf{q},\mathbf{q}')W^{xx(jj')\lambda}_{rsn'm'}\\ &\times(\mathbf{q}',0)\left[p^{sj}_{n'}p^{s'j'}_{m'}+\lambda p^{s'j}_{n'}p^{sj'}_{m'}\right]. \quad (12)\end{aligned}$$

The definitions of the coefficients are as follows. $\varepsilon^{sj}_n(\mathbf{q}=0)$ is the exciton energy of excitons with zero center-of-mass momentum, γ_2 is the inverse dephasing time of the radiative transition, Ω_{sj} is ($\hbar$ times) the Rabi frequency associated with bands s and j: $\hbar\Omega_{sj}\equiv-\mathbf{d}_{sj}\cdot\mathbf{E}$, and $\tilde{\phi}^{j*}_n(\mathbf{r}=\mathbf{0})$ is the configuration space exciton wavefunction at the origin of the relative coordinates. $A^{jj'j'}_{nmm'}$ denotes the exciton wavefunction integral associated with Pauli blocking,

$$A^{jj'j}_{nmn'}=\sum_{\mathbf{k}}\phi^{j*}_n(\mathbf{k})\phi^{j'*}_m(\mathbf{k})\phi^{j}_{n'}(\mathbf{k}). \quad (13)$$

$W^{xx(jj'\lambda)}_{nmn'm'}(\mathbf{q},\mathbf{q}')$ is the sum ($\lambda=1$) or difference ($\lambda=-1$) of the direct and exchange exciton-exciton interaction matrix elements, respectively:

$$W^{xx(jj'\lambda)}_{nmn'm'}(\mathbf{q},\mathbf{q}')=W^{c(jj')}_{nmn'm'}(\mathbf{q},\mathbf{q}')+\lambda W^{xc(jj')}_{nmn'm'}(\mathbf{q},\mathbf{q}') \quad (14)$$

$$W^{c(jj')}_{nmn'm'}(\mathbf{q},\mathbf{q}')=V(\mathbf{q}-\mathbf{q}')M^{j}_{nn'}(\mathbf{q}-\mathbf{q}')M^{j'}_{mm'}(\mathbf{q}'-\mathbf{q}) \quad (15)$$

$$\begin{aligned}&W^{xc(jj')}_{nmn'm'}(\mathbf{q},\mathbf{q}')=\\ &\sum_{\mathbf{k}\mathbf{k}'}V(\mathbf{k}-\mathbf{k}')\,\phi^{j*}_n(\mathbf{k}+\alpha(\mathbf{q}-\mathbf{q}'))\,\phi^{j'*}_m(\mathbf{k}'+\beta'\mathbf{q}+\beta\mathbf{q}')\\ &\times\Big[\phi^{j}_{n'}(\mathbf{k})-\phi^{j}_{n'}(\mathbf{k}')\Big]\Big[\phi^{j'}_{m'}(\mathbf{k}+\alpha(\mathbf{q}-\mathbf{q}')+\beta\mathbf{q}+\beta'\mathbf{q}')\\ &-\phi^{j'}_{m'}(\mathbf{k}'+\alpha(\mathbf{q}-\mathbf{q}')+\beta\mathbf{q}+\beta'\mathbf{q}')\Big]\cdot \quad (16)\end{aligned}$$

$W^{c(jj')}$ and $W^{xc(jj')}$ are the Fourier transforms (relative to the exciton center-of-mass coordinates) of the direct and exchange exciton interactions in *e.g.* [39,40]. We note that through the exchange term, optically inactive exciton states are also included in the eigenfunction basis here. In the direct term, the so-called excitonic transition matrix elements is defined by

$$M^{j}_{nn'}(\mathbf{q})=\sum_{\mathbf{k}}\phi^{j*}_n(\mathbf{k})\Big[\phi^{j}_{n'}(\mathbf{k}+\beta\mathbf{q})-\phi^{j}_{n'}(\mathbf{k}-\alpha\mathbf{q})\Big]\cdot \quad (17)$$

The zero-$\mathbf{q}$ limit of $W^{xx(jj')}$ gives the Hartree-Fock matrix element: $\lambda V^{\mathrm{HF}(jj')}_{nmn'm'}=W^{xx(jj'\lambda)*}_{n'm'nm}(0,0)$.

Equation (12) for $b^{sjs'j'\lambda}_{nm}(\mathbf{q})$ is essentially an inhomogeneous Schrödinger equations for the two-electron-two-hole system in the two-exciton basis. The effective two-exciton Hamiltonian is

$$\begin{aligned}H^{xx(jj'\lambda)}_{nmn'm'}(\mathbf{q},\mathbf{q}') &= \Big(\varepsilon^{sj}_n(\mathbf{q})+\varepsilon^{sj'}_m(\mathbf{q})\Big)\,\delta_{nn'}\delta_{mm'}\delta_{\mathbf{q},\mathbf{q}'}\\ &+\sum_{rs\mathbf{k}}\Big(1-\lambda S^{jj'}\Big)^{-1}_{nmrs}(\mathbf{q},\mathbf{k})W^{xx(jj'\lambda)}_{rsn'm'}(\mathbf{k},\mathbf{q}') \quad (18)\end{aligned}$$

which contains the overlap matrix again as a result of the nonorthogonality of the antisymmetrized two-exciton wavefunctions. If we consider the limit of infinite hole mass and restrict the expansion to 1s-functions only, the kinetic energy vanishes and the interaction as well as the overlap matrix depend on $\mathbf{q}-\mathbf{q}'$ only. For a finite hole mass, however, the interaction remains nonlocal and also nonhermitian, which will be discussed later. Another phenomenological dephasing rate, γ_b, has been introduced, which represents (rather crudely) the dephasing effects of the environment, *e.g.* phonons and other excitons, on the correlated propagation of the two coherent excitons. One may write γ_b in the form $\gamma_b=2\gamma_2+\delta$, where $2\gamma_2$ represents the dephasing suffered by the two excitons individually between two scatterings off each other, and δ represents dephasing processes that irreducibly involve both excitons. Setting γ_b to $2\gamma_2$, as we do in this paper, amounts to assuming that the irreducibly two-exciton dephasing processes are negligible. The contributions to γ_b from other excitons present in the system are of higher order in the exciting field and are therefore negligible in the $\chi^{(3)}$ regime considered in this paper. A quantitative estimate of γ_b is beyond the scope of this paper.

$$G^{(jj'\lambda)}_{nmn'm'}(\Omega)=\frac{1}{2}\sum_{Jn''m''n'''m'''\mathbf{q}\mathbf{q}'}\frac{\left[W^{xx(jj'\lambda)*}_{n''m''nm}(\mathbf{q},\mathbf{0})\zeta^{(jj'\lambda)J}_{n''m''}(\mathbf{q})\right]\left[\zeta^{(jj'\lambda)J*}_{n'''m'''}(\mathbf{q}')\,W^{xx(jj')\lambda}_{n'''m'''n'm'}(\mathbf{q}',\mathbf{0})\right]}{\hbar\Omega-\epsilon^{(jj'\lambda)}_{J}+\mathrm{i}\gamma_b}\,. \tag{27}$$

Equation (12) may be solved formally to give the biexcitonic amplitude as

$$b^{sjs'j'\lambda}_{nm}(\mathbf{q},t)=\int_{-\infty}^{\infty}\mathrm{d}t'\sum_{rsn'm'\mathbf{q}'}\tilde{\mathcal{G}}^{(jj'\lambda)}_{nmrs}(\mathbf{q},\mathbf{q}',t-t')\times W^{xx(jj')\lambda}_{rsn'm'}(\mathbf{q}',\mathbf{0})\left[p^{sj}_{n'}(t')\,p^{s'j'}_{m'}(t')+\lambda p^{s'j}_{n'}(t')\,p^{sj'}_{m'}(t')\right], \tag{19}$$

where the retarded two-exciton propagator is

$$\tilde{\mathcal{G}}^{(jj'\lambda)}_{nmrs}(\mathbf{q},\mathbf{q}',t-t')=\frac{1}{2\mathrm{i}\hbar}\theta(t-t')\sum_{r's'\mathbf{q}''}\left[\mathrm{e}^{-\frac{\mathrm{i}}{\hbar}[H^{xx(jj'\lambda)}-\mathrm{i}\gamma_b](t-t')}\right]_{nmr's'}\times(\mathbf{q},\mathbf{q}'')\left(1-\lambda S^{jj'}\right)^{-1}_{r's'rs}(\mathbf{q}'',\mathbf{q}')\,. \tag{20}$$

Here again $\tilde{\mathcal{G}}^{(jj'\lambda)}$, $H^{xx(jj'\lambda)}$ are matrices in the basis $(n,m,\mathbf{q})$. Substituting the expression equation (19) into equation (11) eliminates $b^{sjs'j'\lambda}_{nm}(\mathbf{q})$ in favor of a closed equation for p^{sj}_{n}: the last term of equation (11) would become

$$\mathrm{i}\hbar\frac{\mathrm{d}}{\mathrm{d}t}p^{sj}_{n}(t)\mid_{\mathrm{corr.}}\equiv\sum_{s'j'\lambda mn'm'}p^{s'j'*}_{m}(t)\times\int_{-\infty}^{\infty}\mathrm{d}t'\tilde{G}^{(jj'\lambda)}_{nmn'm'}(t-t')\left[p^{sj}_{n'}(t')p^{s'j'}_{m'}(t')+\lambda p^{s'j}_{n'}(t')p^{sj'}_{m'}(t')\right], \tag{21}$$

$$\tilde{G}^{(jj'\lambda)}_{nmn'm'}(t-t')=\sum_{n''m''n'''m'''\mathbf{q}\mathbf{q}'}W^{xx(jj'\lambda)*}_{n''m''nm}(\mathbf{q},\mathbf{0})\tilde{\mathcal{G}}^{(jj'\lambda)}_{n''m''n'''m'''}\times(\mathbf{q},\mathbf{q}',t-t')\,W^{xx(jj')\lambda}_{n'''m'''n'm'}(\mathbf{q}',\mathbf{0})\,. \tag{22}$$

As can be seen, the retarded Coulomb correlational dynamics between the two excitons is governed by the kernel $\tilde{G}^{(jj'\lambda)}_{nmn'm'}(t-t')$. Its spectral properties, given by its Fourier transform

$$G^{(jj'\lambda)}_{nmn'm'}(\Omega)=\frac{1}{2}\sum_{n''m''n'''m'''\mathbf{q}\mathbf{q}'}W^{xx(jj'\lambda)*}_{n''m''nm}(\mathbf{q},\mathbf{0})\times\left[\frac{1}{\hbar\Omega-H^{xx(jj'\lambda)}+\mathrm{i}\gamma_b}\left(1-\lambda S^{jj'}\right)^{-1}\right]_{n''m''n'''m'''}\times(\mathbf{q},\mathbf{q}')\,W^{xx(jj')\lambda}_{n'''m'''n'm'}(\mathbf{q}',\mathbf{0})\,, \tag{23}$$

is the object of main interest in this paper.

The exponential of $H^{xx(jj'\lambda)}$, or the inverse of $\hbar\Omega-H^{xx(jj'\lambda)}+\mathrm{i}\gamma_b$, may be computed by, among other ways, diagonalization. The construction is standard except for the slight complication that $H^{xx(jj'\lambda)}$ is not a hermitian matrix in the $(n,m,\mathbf{q})$ basis. This loss of 'manifest' hermiticity is again an artifact of the basis: the matrix of the same Hamiltonian in the electron and hole single-particle momentum basis (**k**-basis for short) is Hermitian. The two representations, exciton $(n,m,\mathbf{q})$ and fermionic (**k**-), of the $(2e$–$2h)$ Hamiltonian must of course have the same (real) eigenvalue spectrum. Taking the orthogonality relation of the eigenvectors in the **k**-basis and transforming to the $(n,m,\mathbf{q})$ basis, one can easily show that the eigenvectors in the $(n,m,\mathbf{q})$ basis are 'orthogonal relative to S'. Explicitly, let $\{\epsilon^{(jj'\lambda)}_{J}\}$ and $\{\zeta^{(jj'\lambda)J}_{nm}(\mathbf{q})\}$ be respectively the set of eigenvalues and eigenvectors, labeled by J, of $H^{xx(jj'\lambda)}$ for given j,j',λ. Then

$$\sum_{nm\mathbf{q},n'm'\mathbf{q}'}\zeta^{(jj'\lambda)J*}_{nm}(\mathbf{q})\left(1-\lambda S^{jj'}\right)_{nm,n'm'}\times(\mathbf{q},\mathbf{q}')\,\zeta^{(jj'\lambda)J'}_{n'm'}(\mathbf{q}')=\delta_{JJ'}. \tag{24}$$

For the following construction of $\tilde{\mathcal{G}}^{(jj'\lambda)}$, we simplify the notation to $a\equiv(n,m,\mathbf{q})$. Let $\mathcal{U}^{jj'\lambda}$ denote the matrix constructed by assembling the eigenvectors in columns: $\mathcal{U}^{jj'\lambda}_{aJ}=\zeta^{(jj'\lambda)J}_{a}$. Then the two-exciton propagator in equation (20) is given by:

$$\tilde{\mathcal{G}}^{(jj'\lambda)}_{aa'}(t-t')=\frac{1}{2\mathrm{i}\hbar}\theta(t-t')\sum_{Ja''}\mathrm{e}^{-\frac{\mathrm{i}}{\hbar}[\epsilon^{(jj'\lambda)}_{J}-i\gamma_b](t-t')}\times\left[\mathcal{U}^{jj'\lambda}\right]_{aJ}\left[\mathcal{U}^{jj'\lambda}\right]^{-1}_{Ja''}\left(1-\lambda S^{jj'}\right)^{-1}_{a''a'} \tag{25}$$

and its Fourier transform by

$$\mathcal{G}^{(jj'\lambda)}_{aa'}(\Omega)=\frac{1}{2}\sum_{Ja''}\frac{\left[\mathcal{U}^{jj'\lambda}\right]_{aJ}\left[\mathcal{U}^{jj'\lambda}\right]^{-1}_{Ja''}}{\hbar\Omega-\epsilon^{(jj'\lambda)}_{J}+\mathrm{i}\gamma_b}\left(1-\lambda S^{jj'}\right)^{-1}_{a''a'}=\frac{1}{2}\sum_{J}\frac{\zeta^{(jj'\lambda)J}_{a}\zeta^{(jj'\lambda)J*}_{a'}}{\hbar\Omega-\epsilon^{(jj'\lambda)}_{J}+\mathrm{i}\gamma_b}. \tag{26}$$

The last equality is valid because $\mathcal{U}^{jj'\lambda}$, though not unitary, obeys the relation $[\mathcal{U}^{jj'\lambda}]^{-1}=[\mathcal{U}^{jj'\lambda}]^{\dagger}(1-\lambda S^{jj'})$. We note, however, that the equivalence of two forms strictly holds when the problem is solved in the entire basis space; it may be spoiled under truncation of the basis or other approximations. With equation (26), the retarded exciton-exciton correlation kernel in frequency space equation (23) is

See equation (27) above.

The calculation of $G^{(jj'\lambda)}_{nmn'm'}(\Omega)$ may be simplified if we assume that the Hamiltonian equation (18) is invariant under rotation in the quantum well's plane. In this case, one can advantageously work in the angular momentum basis conjugate to the angle coordinate of $\mathbf{q}$: it is shown in Appendix A that the four-fermion Hamiltonian can be decoupled into blocks labeled by the total (z-component of the) angular momentum.

2.2 The 1s exciton-exciton T-matrix

While the above equations are still the most general equations in the coherent $\chi^{(3)}$-regime, owing to the fact that there are infinitely many internal exciton quantum numbers, they are in general much more difficult to solve than the equations written in a straightforward one-particle momentum-space formulation. The computational benefit of the exciton representation lies in the fact that, under certain conditions, the 1s-excitons dominate the optical response and, therefore, are the only contributions to the above equation that need to be taken into account. In the following we will consider the case in which the 1s-excitons may be assumed to be dominant. Specifically, we assume resonant 1s-exciton excitation with light pulses whose spectrum covers only the 1s-hh-exciton. Even in this case, when all three 'source' interband polarizations in equation (21) are restricted to 1s, we can see from equation (22) that during the two excitons' propagation from t to t', they may still scatter off each other into higher internal states. Equation (27) shows that these higher states' contributions are suppressed to a certain extent by the energy denominator, but the critical dependence is on the size of $W^{xx(jj'\lambda)}_{nm1s1s}(\mathbf{q},\mathbf{0}), n,m \neq 1s$. Estimates shown in the next section will indicate that these contributions from higher exciton intermediate states are indeed quite small. So it is of practical interest to discuss the theory in the approximation where all excitonic quantum numbers are restricted to 1s. In this major simplification, all matrices such as $W^{xx(jj'\lambda)}_{nmn'm'}(\mathbf{q},\mathbf{q}')$ reduce to matrices indexed only by $\mathbf{q}$ and $\mathbf{q}'$. Exciton state labels (n,m,n',m' etc) will be dropped from all symbols, except where noted otherwise, with the understanding that they are all 1s. Moreover, we will restrict ourselves to two parabolic bands, *i.e.*, one conduction band and one heavy-hole valence band: the orbital label j just represents the hole spin projection, taking the values $\pm\frac{3}{2}$. We can then label the interband polarization by the exciton's spin $p_\pm \equiv p^{\mp\frac{1}{2}\pm\frac{3}{2}}$. The 1$s$ exciton wavefunction in our model is $\phi(\mathbf{k}) = \frac{\sqrt{2\pi}a_0}{[1+(a_0k/2)^2]^{3/2}}$, where $a_0 \equiv \frac{\hbar^2\epsilon_b}{{q_e}^2 m_r}$ is the exciton Bohr radius, m_r being the electron-hole reduced mass. Since this wavefunction is independent of j, so are all the system coefficients and matrix elements in the interband polarization's equation of motion.

In this case, equation (11) together with equation (21) are simplified to

$$\begin{aligned}
\mathrm{i}\hbar\frac{\mathrm{d}}{\mathrm{d}t}p_\pm(t) &= (\varepsilon(0)-\mathrm{i}\gamma_2)p_\pm(t) - \Omega_\pm(t)\tilde{\phi}^*(\mathbf{0}) \\
&\quad + 2\Omega_\pm(t)A^{\mathrm{PSF}}p_\pm(t)p^*_\pm(t) + V^{\mathrm{HF}}p_\pm(t)p_\pm(t)p^*_\pm(t) \\
&\quad + 2p^*_\pm(t)\int_{-\infty}^{\infty}\mathrm{d}t'\tilde{G}^+(t-t')p_\pm(t')p_\pm(t') \\
&\quad + p^*_\mp(t)\int_{-\infty}^{\infty}\mathrm{d}t'\left[\tilde{G}^+(t-t')+\tilde{G}^-(t-t')\right]p_\mp(t')p_\pm(t').
\end{aligned} \tag{28}$$

The phase space filling constant, the HF constant, and the configuration space exciton wavefunction at $\mathbf{r}=\mathbf{0}$ have the explicit expressions

$$A^{\mathrm{PSF}} = \sum_{\mathbf{k}}\phi^*(\mathbf{k})\phi^*(\mathbf{k})\phi(\mathbf{k}) = \frac{4\sqrt{2\pi}}{7}a_0 \tag{29}$$

$$\begin{aligned}
V^{\mathrm{HF}} &= 2\sum_{\mathbf{k}\mathbf{k}'}V(\mathbf{k}-\mathbf{k}')|\phi(\mathbf{k})|^2\phi(\mathbf{k}')\left\{\phi^*(\mathbf{k})-\phi^*(\mathbf{k}')\right\} \\
&= 2\pi\left(1-\frac{315\pi^2}{4096}\right)a_0^2E_b \sim 1.52a_0^2E_b,
\end{aligned} \tag{30}$$

$$\tilde{\phi}^*(\mathbf{0}) = \sum_{\mathbf{k}}\phi^*(\mathbf{k}) = \frac{2\sqrt{2}}{a_0\sqrt{\pi}} \tag{31}$$

where $E_b \equiv \frac{2\hbar^2}{m_r{a_0}^2}$ is the 2D exciton Rydberg. The quantities $H^{xx\lambda}, W^{xx\lambda}, G^\lambda$, and S, defined in the previous subsection, are all reduced to matrices in $\mathbf{q}$. As explained in Appendix A, angular momentum conservation reduces the construction of $\tilde{G}^\lambda$ to a one-dimensional problem, involving only the radial coordinate of $\mathbf{q}$. The numerical solution of this reduced problem is discussed in the next section.

In the remainder of this section, we will interpret the two-exciton propagation in equation (28) in terms of the concepts in general scattering theory in two dimensions. To this end, we consider the following combinations in the two total electron spin channels: $\mathcal{T}^\lambda(\Omega) \equiv \lambda V^{\mathrm{HF}} + 2G^\lambda(\Omega)$. Noting that $\lambda V^{\mathrm{HF}} = W^{xx(\lambda)*}(\mathbf{0},\mathbf{0})$ and equation (23), we can write $\mathcal{T}^\lambda(\Omega)$ explicitly as:

$$\begin{aligned}
\mathcal{T}^\lambda(\Omega) &= W^{xx(\lambda)*}(\mathbf{0},\mathbf{0}) + \sum_{\mathbf{q}\mathbf{q}'}W^{xx(\lambda)*}(\mathbf{q},\mathbf{0}) \\
&\quad\times\left[\frac{1}{\hbar\Omega - H^{xx(\lambda)} + \mathrm{i}\gamma_b}(1-\lambda S)^{-1}\right]_{\mathbf{q}\mathbf{q}'} W^{xx(\lambda)}(\mathbf{q}',\mathbf{0}).
\end{aligned} \tag{32}$$

We can compare the structure of this equation with that of the Lippmann-Schwinger equation (see *e.g.* [31]) for the scattering amplitude or T-matrix of an elastic collision between two particles. For convenience of reference, we include a short recap of the latter here. Take a generic Hamiltonian $H^{pp} = H_0^{pp} + V$ for two particles where H_0^{pp} is the kinetic energy and V is a short-ranged, possibly nonlocal, potential defined in the basis of relative momentum eigenstates. We work in the center-of-mass frame in which the kinetic energy matrix element between states

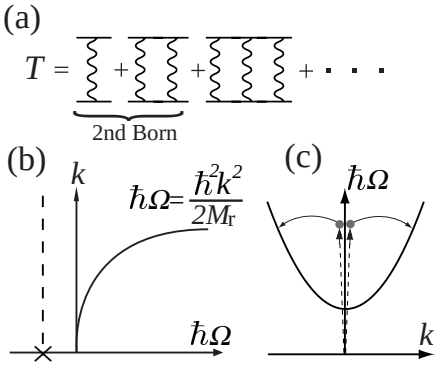

Fig. 1. (a) Schematic visualization of the T-matrix. The squiggly lines represent the interaction. (b) Schematic of the domain of the T-matrix. The cross and dashed line indicate the position of the biexciton pole. (c) Schematic of the creation of coherent excitons as virtual particles and their transition into incoherent excitons as real populations.

of relative momenta $\mathbf{k}$ and $\mathbf{k}'$ is $H_0^{pp}(\mathbf{k},\mathbf{k}') = \delta_{\mathbf{k},\mathbf{k}'}\frac{\hbar^2k^2}{2M_r}$, M_r being the reduced mass of the two body system. The Lippmann-Schwinger equation for the (off-energy-shell, retarded) T-matrix element of energy $\hbar\Omega$ between states of relative momenta $\mathbf{k}$ and $\mathbf{k}'$ is

$$T_{LS}(\mathbf{k},\mathbf{k}',\Omega) = V(\mathbf{k},\mathbf{k}') + \sum_{\mathbf{q}\mathbf{q}'} V(\mathbf{k},\mathbf{q})\left[\frac{1}{\hbar\Omega - H^{pp} + \mathrm{i}\eta}\right]_{\mathbf{q}\mathbf{q}'} V(\mathbf{q}',\mathbf{k}') \quad (33)$$

$$= V(\mathbf{k},\mathbf{k}') + \sum_{\mathbf{q}\mathbf{q}'} V(\mathbf{k},\mathbf{q})\left[\frac{1}{\hbar\Omega - H_0^{pp} + \mathrm{i}\eta}\right]_{\mathbf{q}\mathbf{q}'} \times T_{LS}(\mathbf{q}',\mathbf{k}',\Omega), \qquad \eta \searrow 0. \quad (34)$$

The second equality, equation (34), defines *via* iteration a perturbation theory for $T_{LS}(\mathbf{k},\mathbf{k}',\Omega)$ which is schematically represented in Figure 1a. *via* the Lippmann-Schwinger equation, the T-matrix is in general defined for all values of its argument $(\mathbf{k},\mathbf{k}',\Omega)$, even for complex Ω. The magnitude squared of its value on the *energy shell*, *i.e.* $|\mathbf{k}| = |\mathbf{k}'| = k$ and $\hbar\Omega = \frac{\hbar^2k^2}{2M_r}$, yields the differential cross section of elastic scattering between the directions $\hat{\mathbf{k}}$ and $\hat{\mathbf{k}}'$. The relation between the on-shell part of the T-matrix and the more general off-shell part is illustrated in Figure 1b, where the case of principal interest here – forward scattering, $\mathbf{k} = \mathbf{k}'$ – is shown. As is well known, the off-energy-shell T-matrix plays a significant role in the statistical mechanics of quantum many-body systems. In particular, it governs the equilibrium behavior of dilute nonideal quantum gases. We may also interpret the colliding particles as having 'off-energy-shell' initial and final states, *i.e.*, products of single-particle states with well-defined frequency and momentum which however are not related by the free-particle dispersion relation. We refer to these states also as 'virtual' and the on-energy-shell states as 'real'. One more point of interest in this paper is that $-\mathrm{Im}T_{\mathrm{LS}}(\mathbf{k},\mathbf{k},\Omega)$ gives the rate of scattering of two *virtual* particles with relative momentum $\mathbf{k}$ to *real* particles with momentum magnitude $\sqrt{2M_r\hbar\Omega}/\hbar$. The underlying scattering process is schematically shown in Figure 1c. The two off-resonantly created excitons which are not on the exciton-energy dispersion curve, and which correspond to real but transient excitonic polarizations (coherent excitons), scatter *via* exciton-exciton interaction onto the exciton-dispersion. This results in the population of "real" incoherent excitons. The mathematical description of these populations, however, is beyond the $\chi^{(3)}$-regime and therefore not part of the analysis in this paper. The $\chi^{(3)}$-regime contains only information about the scattering out of the state of two virtual (coherent) excitons, not the scattering into specific real excitons. Note that our distinction between virtual and real particles is based on the assumption of zero linewidth (or, at least, zero spectral overlap between the light spectrum and the zero-momentum exciton spectrum), and that it is only valid for the case of off-resonant excitation.

Comparing equation (32) with equation (33), we see that $\mathcal{T}^\lambda(\Omega)$ in the zero damping limit may be interpreted as the forward ($\hat{\mathbf{k}} = \hat{\mathbf{k}}'$) off-shell scattering amplitude, or T-matrix, for zero momentum and energy $\hbar\Omega$ with caveats stemming from the use of the antisymmetrized two-exciton basis: the presence of the overlap matrix S, and the nonhermiticity of the interaction $W^{xx(\lambda)}$. We will present a numerical analysis in the next section that shows, in spite of these complications, $\mathcal{T}^\lambda(\Omega)$ still behaves like a typical two-particle scattering amplitude (as defined by Eq. (33). For example, it is known that, in *two* dimensions, the zero-momentum off-energy-shell T-matrix for a generic hermitian, short-ranged, even nonlocal potential behaves asymptotically at low energies as [33] $T_{LS}(\mathbf{0},\mathbf{0},z) \approx -\frac{2\pi\hbar^2}{M_r}\frac{1}{\ln[(-z)/\varepsilon_c]}$, where z is in general complex. This asymptotic behavior holds for $|z| \ll \varepsilon_c$, where ε_c is an energy scale that depends on the specific $V(\mathbf{k},\mathbf{k}')$ in each problem. In the exciton terminology and units used here, this asymptotic formula reads:

$$T_{LS}(\mathbf{0},\mathbf{0},\hbar\Omega+\mathrm{i}\gamma_b) \approx -\frac{2\pi\alpha(1-\alpha)}{\ln(-(\hbar\Omega - 2\varepsilon(\mathbf{0}) + \mathrm{i}\gamma_b)/\varepsilon_c)} {a_0}^2 E_b. \quad (35)$$

We will see that $\mathcal{T}^\lambda(\Omega)$ follows this behavior quite well. With this and other results in the next section, we interpret $\mathcal{T}^\lambda(\Omega)$ as the zero-momentum off-energy-shell T-matrix for two colliding excitons with total electron spin 1 ($\lambda = 1$) or 0 ($\lambda = -1$).

The role of the T-matrix in the $\chi^{(3)}$ equation equation (28) is slightly more explicit if we go to the channels of parallel (++) and opposite (+−) exciton spins: $T^{++}(\Omega) \equiv \mathcal{T}^+(\Omega)$ and $T^{+-}(\Omega) \equiv (\mathcal{T}^+(\Omega) + \mathcal{T}^-(\Omega))/2$. The three terms involving interactions (HF and correlations) between the two excitons in equation (28) can be written compactly in terms of the inverse Fourier transforms of $T^{++}(\Omega)$ and $T^{+-}(\Omega)$:

$$p_\pm^*(t)\int_{-\infty}^{\infty}\mathrm{d}t'\tilde{T}^{++}(t-t')p_\pm(t')p_\pm(t') + p_\mp^*(t) \times \int_{-\infty}^{\infty}\mathrm{d}t'\tilde{T}^{+-}(t-t')p_\mp(t')p_\pm(t'). \quad (36)$$

Roughly, the two excitons are created with energies and momenta obeying the photon dispersion relation instead of that of real excitons. That is why their scattering is described by the off-energy-shell part of the T-matrix instead of the usual on-shell part. In the statistical mechanics of dilute gases, it is the correlation with surrounding particles that modifies the energy-momentum dispersion relation of a particle. From these considerations, coherent nonlinear optics can be seen as a probe on the off-shell excitonic T-matrix, which can then be used to estimate thermodynamic quantities of a dilute low-temperature exciton gas. Moreover, a theoretical model validated by comparison with these experiments can also yield the on-shell part of the excitonic T-matrix from which excitation-induced dephasing and relaxation rates can be obtained.

3 Estimation of off-energy-shell T-matrix

In the previous section we reviewed the DCT equations in the exciton basis. We have seen that in this formalism the (spin-dependent) four-particle correlation terms can be represented as the off-energy-shell forward scattering (or T-) matrix element for two (virtual) particles. Of course, in the exact four-fermion theory, the entire exciton basis set, $1s$ and higher, has to be included as intermediate states in the calculation of the T-matrix. In other words, even though the external light field creates only (virtual) $1s$-excitons with zero center-of-mass momentum, the (virtual) scattering processes include states that are not restricted to $1s$ or zero center-of-mass momentum. From a practical point of view, it is relatively easy to include nonzero center-of-mass momentum $1s$-exciton states as intermediate states, but it is very difficult to include higher exciton states ($2s$, $2p$, ..., and exciton-continuum states).

Since we can, for practical reasons, evaluate the $\chi^{(3)}$ theory only with arbitrary center-of-mass momentum $1s$-exciton states as intermediate states (we call it the "$1s$-approximation"), we have to address the issue of how good this approximation is. Unfortunately, there exist no simple criterion based on small parameter. Therefore, a rigorous analysis of the quality of the $1s$-approximation could only be achieved by a comparison with the full, non-approximate solution. While this is not feasible, it is still instructive to discuss a number of individual aspects of the theory that are related to the influence of higher exciton states and the mathematical consequences of the $1s$-approximation. In the following, we will first investigate the contribution of higher exciton states to the interaction matrix elements. We will also discuss mathematical artefacts of the interaction matrix elements in the $1s$-approximation. We will discuss the role of the exciton overlap matrix element within the $1s$-approximation and possible artefacts related to it. Evaluating the theory within the $1s$-approximation, we study the quality of the biexciton state obtained through direct matrix diagonalization. Finally, we will discuss the low-energy behavior of the T-matrix in the $1s$-approximation and compare it to results well-known for two-particle correlations in 2-dimensional systems in which the interaction potential is short-ranged.

3.1 Contributions from higher exciton states

In this section, we study the influence of interaction matrix elements $W_{nm,n'm'}$ involving exciton states other than $1s$. Since each term in the T-matrix summation that we obtained in Section 2 begins and ends with the optically excited (virtual) excitons (*i.e.*, $1s$-excitons with $\boldsymbol{q} = 0$), we focus on matrix elements that couple the optically excited $1s$-excitons to higher states: $W_{nm,1s1s}$; in other words, we look at the beginning or, equivalently, the end of each ladder-type diagram (*cf.* Fig. 1a). We argue that, if these matrix elements are much smaller than the ones used in the $1s$-approximation, $W_{1s1s,1s1s}$, then the $1s$-approximation is valid unless some other matrix elements $W_{nm,n'm'}$ (with $n, m, n', m' \neq 1s$) overcompensate the effects of the small $W_{nm,1s1s}$ (with $n, m \neq 1s$) elements. While we cannot rule that out, we don't believe that to be likely. As for the matrix elements $W_{nm,1s1s}$ (with $n, m \neq 1s$), we should ideally study all possible quantum numbers n and m. Again, for practical reason, we restrict ourselves to a few examples for n and m. We believe these examples to be representative and we believe that other matrix elements are likely to be smaller than the ones we study here. To be concrete, we evaluate $W_{nm,1s1s}$ for n, m assuming the values in the set $\{1s,\ 2s,\ 2p_x,\ 2p_y\}$.

As a figure of merit regarding the influence of higher exciton states on $W^{\lambda}_{nm,1s1s}(\mathbf{q}, \mathbf{q}')$, we plot in Figure 2 the integrals $\sum_{\mathbf{q}} |W^{xx\lambda}_{nm,1s1s}(\mathbf{q}, 0)|^2$, as a function of electron hole mass ratio. In the numerical integration, we limit the range of $q = |\mathbf{q}|$ to 66 a_0^{-1} (where a_0 is the exciton Bohr radius), and use a step size of 0.2 between 0 and 6, and 2.50 between 6 and 66. The step size in the azimuth angle was taken to be $\pi/16$.

As can be seen from Figure 2, the $(m, n) = (1s,1s)$ contributions are always dominant in this figure of merit. Only a small number of individual contributions from higher exciton states reach the level of a few percent (none greater than 7%) of that from $(1s,1s)$ state for both the singlet and triplet channels. The others are much smaller. Therefore, we believe that the neglect of higher exciton states as intermediate scattering states in the T-matrix is a valid approximation provided that only $1s$-excitons are optically excited. In other words, if we look at a contribution to the T-matrix with, say, n interaction lines, and we compare such a contribution that contains only $1s$-states as intermediate states with a contribution that contains two transitions between $1s$ and $2s$ (or $2p$), *i.e.*, the two ends of that contribution, as well as intermediate transitions from, say $2p$ to $3s$, we can assume that the latter is smaller by about one order of magnitude than the former. This is true if the intermediate transitions (like, for example, the $2p$-to-$3s$ transition) is not much larger than the intermediate transitions in the T-matrix that has only $1s$-to-$1s$ transitions. This assumption, albeit not proven, seems at least reasonable.

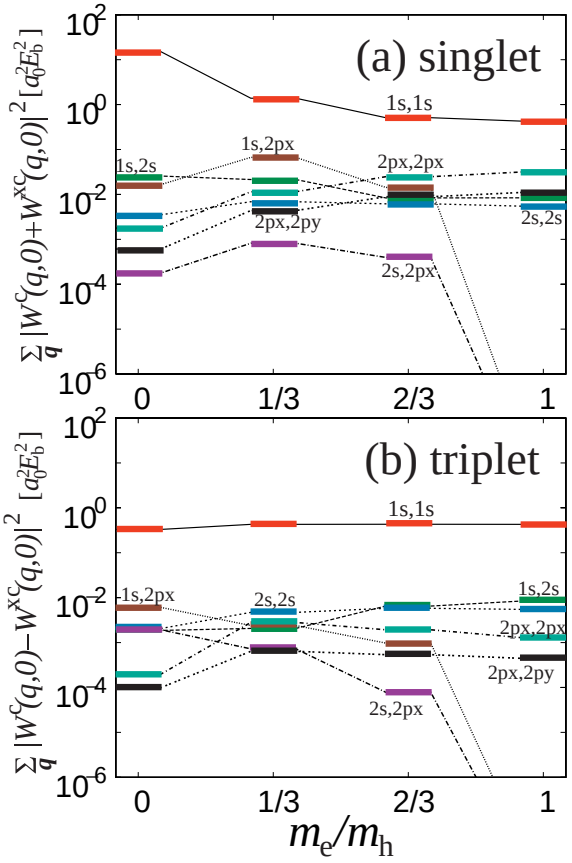

Fig. 2. The contributions from higher exciton states as a function of electron-hole mass ratio. Upper panel: singlet channel. Lower panel: triplet channel. The intermediate states (m,n) are indicated in the figures.

Although the sizes of individual matrix elements $W_{nm,1s1s},(n,m)\neq(1s,1s)$ are small, one needs to sum over an infinity of these intermediate states. The total non-1s correction is thus a result of competition, for increasing intermediate-state energies, between a growing density of states and the decay of the transition matrix elements squared. At present we are not able to give a rigorous analysis of this point. From the trend of those $W_{nm,1s1s}$ that we have calculated, we note that the decay is probably sufficiently fast to cut off the sum over states effectively. An additional factor favoring suppression is the energy denominator in the T-matrix (for example, Eq. (26)). Apart from this direct estimate of higher order contributions, the validity of the neglect of higher intermediate states can be inferred from certain final results of the theory, for example from a comparison of the biexciton binding energy obtained within this approximation with other theories, notably variational approaches (*cf.* Sect. 3.4).

A recent work [13,14] examining the importance of higher (non-1s) exciton states concluded that, as intermediate states in a 'renormalized' Hamiltonian in the 1s subspace, the higher states are crucial for the polarization dependence of the third-order optical responses even when only 1s excitons are excited initially. This conclusion contradicts our findings presented above. In the remainder of this subsection, we attempt to present a clear discussion of this issue. In references [13,14] the conclusion is reached in two steps: (i) first a renormalized exciton-exciton Hamiltonian in the 1s subspace is derived, including the effect of higher exciton states in second-order perturbation theory, (ii) the resulting renormalized Hamiltonian is shown to give a microscopic foundation to a phenomenological bosonic Hamiltonian which was used earlier [17] to explain the polarization dependencies of four-wave-mixing measurements on a quantum-well microcavity. The quantitative estimate in references [13,14] point to important renormalization contributions to the 1s Hamiltonian from the non-1s states, and the parameter values are quantitatively consistent with those obtained by fitting the experiment in reference [17]. We examine this finding in detail below.

The 1s Hamiltonian obtained in references [13,14] is characterized by two constants: U is the magnitude of the first-order transition matrix element for 1s-to-1s scattering, and U', the renormalizing term, is the magnitude of the second-order transition matrix element for 1s-to-1s scattering with non-1s states as intermediate states. U is equal to the Hartree-Fock matrix element $V^{\rm HF}$ in equation (30) above. U' is given by (Eq. (43) in Ref. [14]):

$$U'=\frac{1}{\Omega}\sum_{\mathbf{K}\nu\neq 1s}\frac{|g_\nu(\mathbf{K})|^2}{2(E_\nu+\mathbf{K}^2/2M)-2E_{1s}} \tag{37}$$

$$\begin{aligned} g_\nu(\mathbf{K})=\sum_{\mathbf{p},\mathbf{p}'}V(\mathbf{p}-\mathbf{p}'+\mathbf{K})\,\{&-\phi^*_{1s}(\mathbf{p})\phi^*_{1s}(\mathbf{p}')\phi_\nu(\mathbf{p})\phi_\nu(\mathbf{p}')\\ &+2\phi^*_{1s}(\mathbf{p})\phi^*_{1s}(\mathbf{p}-\mathbf{K})\phi_\nu(\mathbf{p})\phi_\nu(\mathbf{p}')\\ &-\phi^*_{1s}(\mathbf{p})\phi^*_{1s}(\mathbf{p}')\phi_\nu(\mathbf{p}-\mathbf{K})\phi_\nu(\mathbf{p}'+\mathbf{K})\}\cdot \end{aligned} \tag{38}$$

The interaction matrix element between co-polarized excitons is then proportional to $(U-U')/2$, while that between counter-polarized excitons is proportional to $-U'$. Transition matrix elements to optically inactive states are also given by combinations of U and U'. In estimating the size of U', references [13,14] restricted the sum over intermediate states to 2p and then made an estimate of the multidimensional momentum integral. The estimate of U' obtained in this way is very close to U, from which it is concluded that renormalization effects from higher states are important and that these could lead to a strong suppression of the effective interaction strength between co-polarized excitons ($(U-U')/2$) relative to that between counter-polarized excitons ($-U'$). It is further noted that if these interaction matrix elements are used in a lowest-order perturbation calculation of the exciton-exciton scattering amplitude in the 1s subspace, the results would fit the experiment in reference [17]. Since these conclusions depend on the size of U', it is important to check the quantitative accuracy of its estimate given in references [13,14]. We have carried out this check by also restricting the intermediate states to 2p and straightforwardly evaluating the six-dimensional momemtum integral numerically. Instead of a value comparable to U, we obtain a U' which is only about 2% of the size of U. (We note that our calculation revealed massive cancellations among the terms in

$g_{\nu=2p}$.) Therefore, based on the same considerations used in [13,14], we found that, when the numerical evaluation of U' is done with a high-precision algorithm, the conclusions should be reversed: the non-1s renormalization term U' appears not to be a significant correction to U for co-polarized excitons, and the interaction matrix element for counter-polarized excitons is much weaker than that for co-polarized excitons. These conclusions on the importance of higher exciton states are in line with our other estimates presented above.

Of course, the fact that U' is small does not imply that the third-order nonlinear responses involving counter-polarized excitons must be weak. Successive rescatterings within the 1s subspace, *i.e.* 1s-excitons, including optically inactive ones with non-zero momenta, must also be considered. Regarding this point, it is instructive to compare the $\chi^{(3)}$ four-wave-mixing susceptibility for counter-polarized pump excitons as calculated in [13,14] to that calculated *via* a second-Born (leading-order) approximation (setting S to zero) to the 1s scattering amplitude equation (32):

$$\chi^{+-(\text{Ref.14})} \sim \sum_{\mathbf{K},\nu=2p} \frac{|g_\nu(\mathbf{K})|^2}{2(E_\nu - E_{1s}) - \hbar^2\mathbf{K}^2/M} \tag{39}$$

$$\chi^{+-(\text{Present})}_{2\text{ndBA}}(\Omega) \sim \frac{1}{2}\sum_{\mathbf{q}} \frac{|W^{xx(+)}(\mathbf{q},0)|^2 + |W^{xx(-)}(\mathbf{q},0)|^2}{\Omega - \hbar^2\mathbf{q}^2/M + \mathrm{i}\gamma_b}\,. \tag{40}$$

In (40), the dominant intermediate states are the (1s) optically inactive states. Our calculations show that the leading-order 1s rescattering contributions to equation (40) are three to four orders of magnitude larger than the renormalizing contributions from the 2p states.

To summarize, our conclusion in this subsection is, there is no indication so far that the contributions from non-1s intermediate states are important for $\chi^{(3)}$ optical responses around the fundamental exciton. Instead, our calculations of the transition matrix elements between (1s, 1s) and selected higher exciton states support the assumption that the 1s truncation is a valid approximation, although a convincing proof on this point is still lacking. This issue can only be satisfactorily resolved when accurate numerical evaluations of the full four-fermion problem and/or a rigorous theoretical analysis are available. In the remainder of the paper, we restrict ourselves to the 1s-approximation.

3.2 Evaluation of the Coulomb matrix elements

The appearance of the exciton-exciton interaction in the inverse propagator is equivalent to a non-perturbative, infinite-order dependence of the T-matrix on the interaction $W^{xx(\lambda)}_{nm,n'm'}(\mathbf{q},\mathbf{q}')$ (*cf.* Fig. 1a). Thus calculation of the T-matrix requires knowledge of the true two exciton scattering wavefunctions and their eigenenergies. As discussed

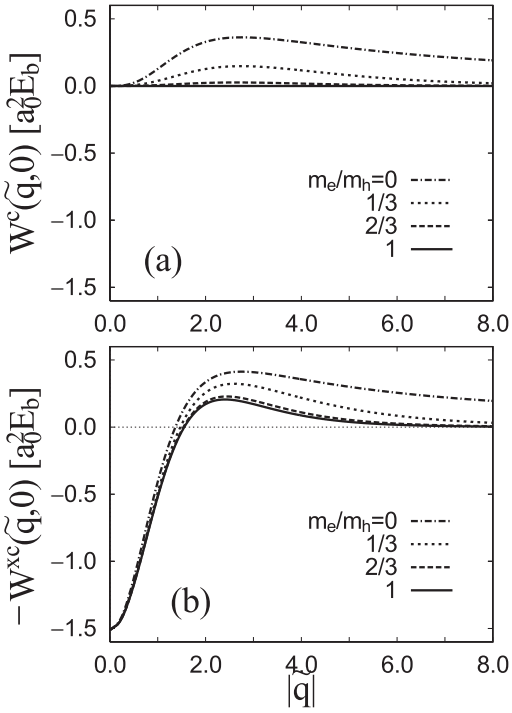

Fig. 3. The direct (a) and exchange (b) exciton-exciton interaction matrix element evaluated for $\tilde{q}' = 0$ (with $\tilde{q} = a_0 q/2$). Here, a_0 (E_b) is the exciton Bohr radius (exciton binding energy).

in the previous section, we believe that the two-exciton states can be restricted to those involving two 1s-excitons with arbitrary center-of-mass momentum, and that higher exciton states can be neglected (under the optical excitation conditions assumed throughout this paper). We have numerically evaluated T by discretizing and diagonalizing angle-averaged matrix elements of $H^{xx(\lambda)}_{1s1s,1s1s}(\mathbf{q},\mathbf{q}')$, and constructed the resolvent *via* eigenfunction expansion. The angle-averaging is a special case of the angular momentum decomposition presented in Appendix A. Specifically, the angle average of $W^\lambda(\mathbf{q},\mathbf{q}') \equiv W^\lambda(q,\theta;q'\theta')$ is given by

$$\bar{W}^\lambda(q,q') = \frac{1}{2\pi}\int_0^{2\pi} \mathrm{d}\theta' W^\lambda(q,0;q'\theta'). \tag{41}$$

Within the 1s-approximation and the assumption of spatially homogeneous and isotropic optical excitation, angle-averaging of the two-exciton Hamiltonian does not constitute an additional approximation (*cf.* Appendix A). Our discretization scheme is briefly discussed in Appendix B.

In our approach to the numerical evaluation of the excitonic T-matrix, it is the computation of the Coulomb matrix elements which is the most time-consuming part. Typically, the quantities W^c and W^{xc} vary strongly for small $\tilde{q}$ (where $\tilde{q} = a_0 q/2$), while for large $\tilde{q}$ they vary little. This can be seen from Figure 3, where we show the potential $W^c(\tilde{q},0)$ and $W^{xc}(\tilde{q},0)$ for various electron-hole mass ratios. The results shown in Figure 3 are in agreement with Figures 1 and 2 of reference [41]. While the plots for $W^{c/xc}(\tilde{q},0)$ give us an overall feeling for the general

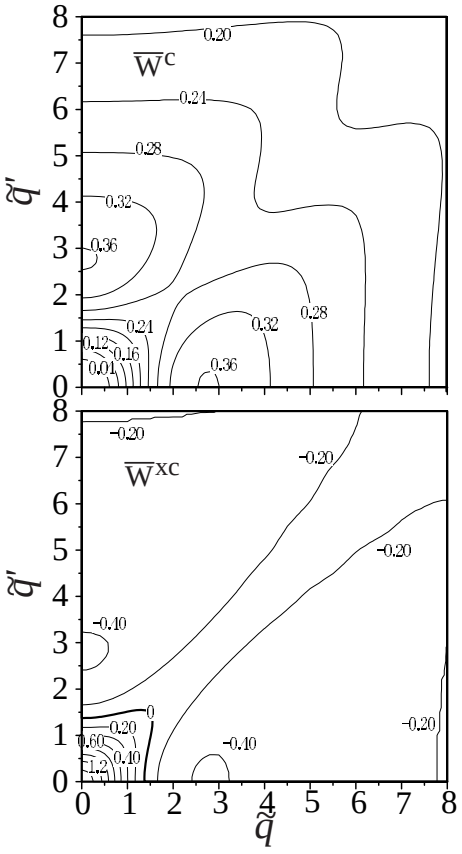

Fig. 4. The angle-averaged exciton-exciton interaction matrix element for $m_\mathrm{e}/m_\mathrm{h} = 0$ in units of $a_0^2 E_b$. $W^\mathrm{c}(0,0) = 0.0$, $W^\mathrm{xc}(0,0) = 1.52$. Upper panel: direct interaction. Lower panel: exchange interaction.

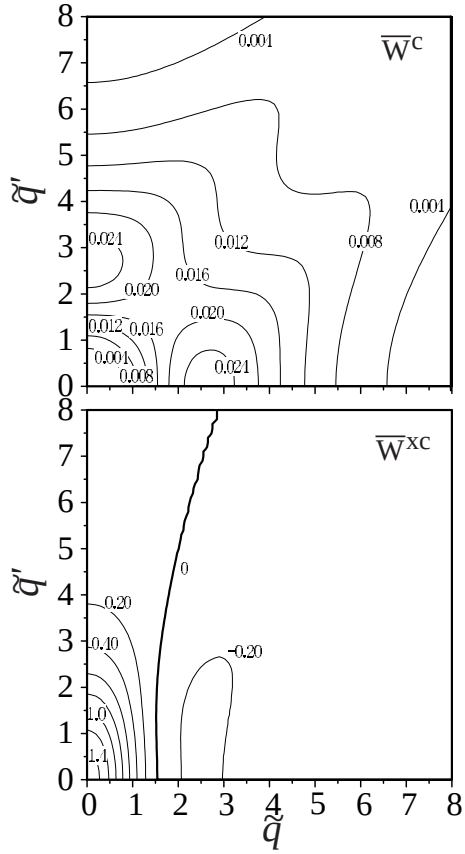

Fig. 5. Same as Figure 4, but for $m_\mathrm{e}/m_\mathrm{h} = 2/3$ (corresponding to GaAs).

behaviour of the potential, in our numerical evaluation of the DCT formalism we need the potential as a function of $\mathbf{q}$ and $\mathbf{q}'$. In our discretization, we take $\Delta\tilde{q} = 0.2$ for the range $0 < |\tilde{q}| < 4$, and $\Delta\tilde{q} = 1.0$ for the range $4 < |\tilde{q}| < 20$. After the calculation of each matrix element of each block matrix specified by (q, q', θ'), we use a 3rd order spline interpolation so that $\Delta\tilde{q} = 5 \times 10^{-3}$. Then we compute the angle average of block matrices. We show the resulting matrices for two mass ratios, $m_\mathrm{e}/m_\mathrm{h} = 0$ and $2/3$, in Figures 4 and 5.

For $m_\mathrm{e}/m_\mathrm{h} = 0$, the matrices W^c and W^{ex} are symmetric with respect to the exchange of q and q'. This reflects the fact that the interaction depends only on $|\,\mathbf{q} - \mathbf{q}'\,|$: the Fourier transform to real space yields a local potential depending only on the distance between the holes. That distance is used as a parameter in the Heitler-London model. On the other hand, in the matrix elements for a finite electron-hole mass ratios, *e.g.* $m_\mathrm{e}/m_\mathrm{h} = 2/3$, the direct part remains local and thus symmetric with respect to the replacement of q and q', while the exchange part is both nonlocal and asymmetric. Thus, if one neglects the factor $(1-\lambda S)^{-1}$ in front of the Coulomb matrix elements, the resulting two-exciton Hamiltonian in the 1s-approximation is in general non-hermitian. In principle, one could therefore expect complex eigenvalues. However, within our computational accuracy, we have found only real eigenvalues.

3.3 The role of the excitonic overlap matrix S

The occurrence of the excitonic overlap matrix S in the two-exciton Hamiltonian, equation (18), presents an additional complication in two respects. First, it simply adds another k-integral to the evaluation of the Coulomb matrix elements. If we would not make any further approximation, such as the 1s-approximation, the S-matrix would certainly have to be taken into account in order to preserve the correct antisymmetry properties of the biexciton amplitude. If, however, one makes additional approximations (in our case it is the 1s-approximation), the resulting S-matrix is only an approximation to the full S-matrix. In this case, one has to make sure that the approximation does not lead to artefacts regarding the S-matrix contributions to the two-exciton Hamiltonian.

The formal issues regarding the occurrence of the S-matrix in the two-exciton Hamiltonian have been discussed in Section 2.1. Within the 1s-approximation, we find that the eigenvector matrix $\mathcal{U}$ (see Eq. (24) and the subsequent discussion) is (to within our numerical accuracy) unitary if the factor $(1 - \lambda S)^{-1}$ in the Coulomb contribution to the two-exciton Hamiltonian is included.

Specifically, the sum of the squared off-diagonal matrix elements of $\mathcal{U}^\dagger\mathcal{U}$ is less than 1% of the sum of the diagonal matrix elements. If we neglect the $(1-\lambda S)^{-1}$ contribution in the two-exciton Hamiltonian, we find that the matrix $\mathcal{U}$ is not strictly unitary, which corresponds to the non-hermiticity of the Coulomb matrix discussed in the previous subsection. Specifically, the deviation from unitarity in the sense of the above-mentioned contribution of off-diagonal matrix elements is about 80% (with maximum about 900%) in the triplet ($\lambda = 1$) and 30% in the singlet ($\lambda = -1$) channel. This also means that inclusion of the $(1-\lambda S)^{-1}$ is necessary for the two-exciton Hamiltonian in the $1s$-approximation to be hermitian.

However, when we look into the behavior of $(1-\lambda S)^{-1}$ in the $1s$-approximation, we face the following problem. We can diagonalize, for example, $(1-\lambda S)$ and take the inverse of its eigenvalues. The quantity $(1-\lambda S)$ is almost diagonal and the eigenvalues are almost unity. Among them, however, a few eigenvalues deviate significantly from unity (for example, we find an eigenvalue of 1.95 for $(1+S)$, and one of 0.05 for $(1-S)$). In particular, in the triplet channel the eigenstate with eigenvalue 1/0.05 leads to a pathological behavior of $(1-S)^{-1}$ in the high energy region of the T-matrix (this will be discussed Fig. 8). Quite generally, if $(1-S)^{-1}$ is very large (in the sense just mentioned), approximations such as the $1s$-approximations may not be trusted. Since, in our case, we can identify the pathological behavior of $(1-S)^{-1}$ with a specific spectral region in the T-matrix, we argue that in spectral regions not affected by this pathological behavior the $1s$-approximation is valid. In general, any approximation affecting S may make results obtained from a calculation that includes S less reliable than results obtained without S. Whether or not this is indeed the case is often difficult to say.

3.4 The biexciton binding energy

In the singlet channel the eigenstates of the interaction Hamiltonian (18) contain a state with negative eigenvalue due to the attractive interaction between two excitons with opposite spin configuration (the bound biexciton state). Numerical results for the biexciton binding energy, $\varepsilon_{\rm xx}$, in units of the exciton Rydberg, E_b, as a function of the electron-hole mass ratio are presented in Figure 6. The solid squares show our results for the case without S. The quantity $\varepsilon_{\rm xx}$ decreases monotonically as $m_{\rm e}/m_{\rm h}$ decreases. The solid line corresponds to the results taken from the literature, namely the variational calculation presented in reference [42]. Since it represents a variational calculation, the true value of the biexciton binding energy should lie above this line. In the region $m_{\rm e}/m_{\rm h} > 0.4$, our results almost agree with that of reference [42]. We also compare with the result in the equal-mass limit obtained from a stochastic variational method (SVM), which may be viewed as the most accurate calculations currently available [43]. In comparison with this our binding energy is slightly lower because we restrict ourselves to the $1s$-exciton basis. On the other hand, the biexciton binding energy obtained with S included in the calculation

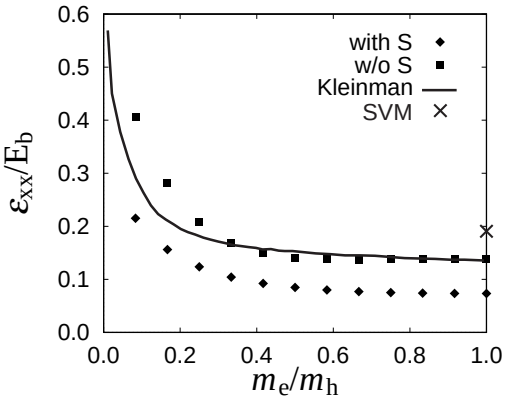

Fig. 6. 2D biexciton binding energy in units of the exciton binding energy as a function of the electron-hole mass ratio with (diamonds) and without (squares) the contribution of the exciton overlap matrix S. The solid line shows the corresponding result of Kleinman's variational calculation (Ref. [42]) and the cross shows the results from the stochastic variational method (Ref. [43]).

is smaller than the one without S. Here is an example where the presence of the matrix $(1+S)^{-1}$ in the two-exciton Hamiltonian amplifies the shortcomings of the $1s$-approximation and a quantitative analysis is better with S being neglected. However, this does not imply that the neglect of $(1+S)^{-1}$ results in a general improvement of the theory.

3.5 The off-energy-shell T-matrix

The truncation to the $1s$ subspace and the inclusion of exchange interaction result in a non-hermitian $W^{xx(\lambda)}$, but we will see that, in spite of this non-hermiticity, our numerical results can be successfully related and compared to the concepts of general scattering theory (*e.g.* [32]). This theory has recently been applied to the analysis of an experiment [44,45]. As was discussed in Section 2.2, the zero-momentum off-energy-shell T-matrix for two colliding particles behaves asymptotically at low energies as [33] $T_{\rm LS}(z) \approx -\frac{2\pi\hbar^2}{M_r}\frac{1}{\ln[(-z)/\varepsilon_{\rm c}]}$, where z is the (complex) energy in the center-of-mass frame and M_r is the reduced mass. We re-write equation (35) as

$$T^{ij}(\hbar\Omega + {\rm i}\gamma_b) \approx -\frac{A^{ij}}{\ln(-(\hbar\Omega - 2\varepsilon(\mathbf{0}) + {\rm i}\gamma_b)/\varepsilon_{\rm c}^{ij})}{a_0}^2 E_b. \tag{42}$$

where $2\varepsilon(\mathbf{0})$ is the continuum edge, and E_b the 2D excitonic Rydberg energy. If the exciton-exciton matrix is hermitian, A^{ij} is $A^{ij} = 2\pi\alpha(1-\alpha)$ (see Eq. (35)), where $\alpha = m_{\rm h}/(m_{\rm e}+m_{\rm h})$. In the following, we will present the T-matrix results we obtain from the DCT approach within the $1s$-approximation and compare it with the Popov formula, equation (42). The comparison will be made quantitative by way of fitting the parameters in the Popov formula to our numerical results.

In Figure 7, we show T^{ij} in the asymptotic region around the continuum edge for a mass ratio of 2/3. When

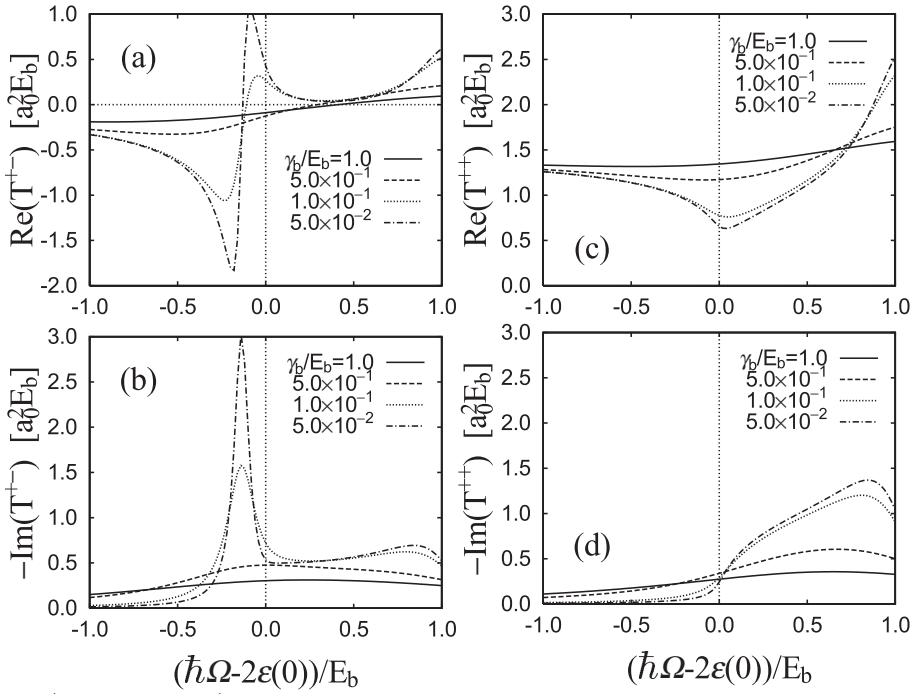

Fig. 7. Exciton-exciton (off-energy-shell) forward scattering amplitude at zero momentum in the counter-circularly (a, b) and co-circularly (c, d) polarization configuration calculated without the contribution of the exciton overlap matrix S. Here $\varepsilon(0)$ is the exciton energy at zero center-of-mass momentum.

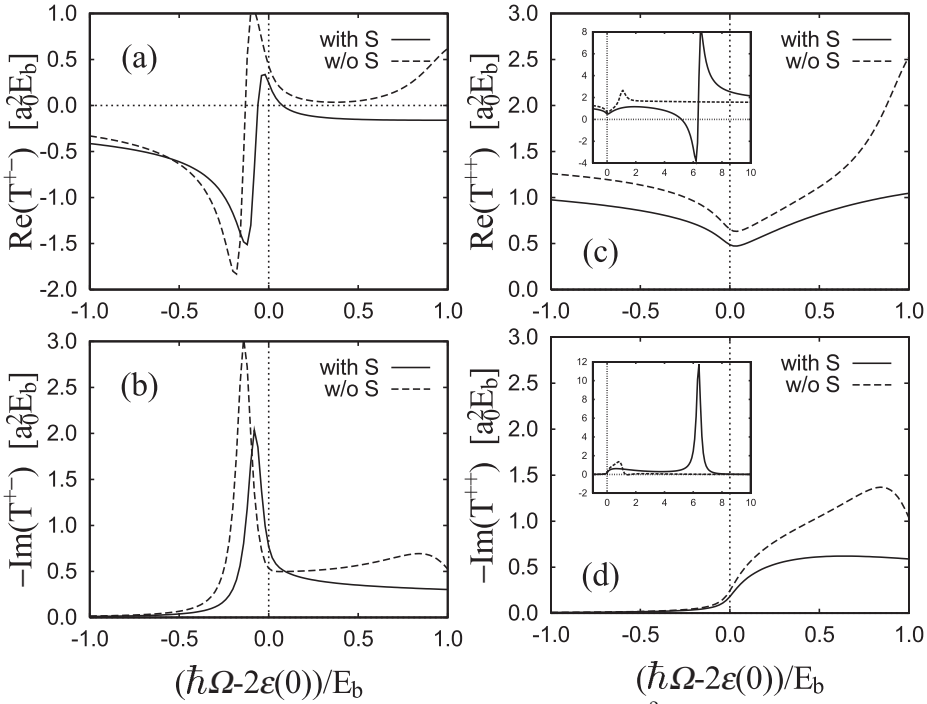

Fig. 8. Same as Figure 7, but for results with (without) S for $\gamma_b/E_b = 5 \times 10^{-2}$ are shown as solid (dashed) lines. The insets show the results on a larger energy scale. See the text Section 3.3.

the dephasing constant γ_b is decreased, our computed T^{ij} indicate or suggest a non-smooth logarithmic behavior of equation (42) and that is independent of the inclusion of S (Fig. 8). Before we explore the similarities to the Popov formula in more detail, we note that the real part of T^{++} shows a minimum at $\hbar\Omega - 2\varepsilon(0) = 0$, and the real part of T^{+-} shows an approximate zero-crossing. This behavior is related to the sum rule of reference [25]. In particular, the sum rule for T^{++} provide an important cancellation between the mean field exchange and correlation effect. To see in more detail whether the sum rule is strictly fulfilled within the $1s$-approximation, we have to study the value of $T^{++}(\hbar\Omega + \mathrm{i}\gamma_b)$ and $T^{+-}(\hbar\Omega + \mathrm{i}\gamma_b)$ for $\hbar\Omega = 2\varepsilon(0)$ in the limit of vanishing γ_b, as only in this limit one can

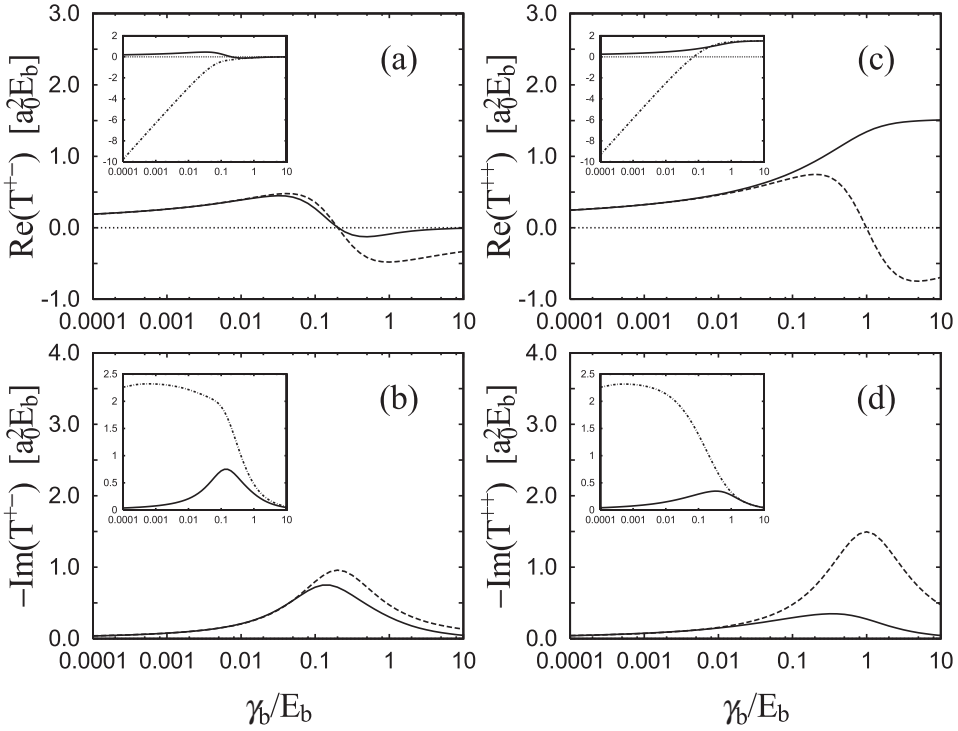

Fig. 9. The zero-energy T-matrices corresponding to Figure 7 for $\hbar\Omega = 2\varepsilon(0)$ as a function of the two-exciton dephasing constant γ_b, calculated without the exciton overlap matrix S for $m_e/m_h = 2/3$. The full numerical result is shown as solid line, and the dashed line shows the corresponding result based on the fitting of Popov's formula to the numerical result. The insets show again the full numerical results (solid line) and the numerical results within the 2nd Born approximation (dash-dotted line).

expect the sum rule to be valid. The solid line in Figure 9 shows the corresponding result without the contribution from the exciton overlap matrix S. Clearly, for small γ_b/E_b, T^{++} and T^{+-} decrease with decreasing γ_b, but very slowly. In contrast, the results from the 2nd Born approximation (dash-dotted lines in the insets) show that in this case the sum rule is not fulfilled at all (see also Ref. [44]). This is especially true in the case with S (not shown).

In order to study in more detail the asymptotic behavior of T^{++} in the limit of vanishing γ_b, we can fit Popov's formula to our full numerical results. If one equates the real and imaginary part of the right hand side of the Popov formula to the numerically given T-matrix in the DCT approach and solves for A^{ij} and ε_c^{ij}, one obtains the values of the fitting parameters A^{ij} and ε_c^{ij}. If the frequency-dependence of the numerically given T-matrix differs from that of the Popov formula, the fitting parameters are no longer constants, but acquire a frequency dependence. In our case, however, we find that this frequency dependence is small as long as one considers only small frequency intervals and as long as one uses sufficiently small damping constants γ_b (smaller than a few times $10^{-3}E_b$). Figure 9 shows that in the limit of vanishing γ_b, the fit matches the numerical results exactly, which means that the asymptotic behavior of the numerical results is given by the $1/\ln(\mathrm{i}\gamma_b)$ behavior of equation (42). This, in turn, allows us to conclude that the asymptotic value of $T^{++}(\hbar\Omega+\mathrm{i}\gamma_b)$ for $\hbar\Omega = 2\varepsilon(0)$ is zero, and that therefore the above-mentioned sum rule is indeed fulfilled.

In Figure 10, we show our numerical computed T^{ij} and the corresponding fit results from the Popov formula in the vicinity of two exciton continuum edge for a mass ratio of 2/3 and $\tilde{\gamma}_b = \gamma_b/E_b = 3 \times 10^{-3}$. The agreement is overall good, even though the biexciton dephasing rate is not extremely small, and the energy interval shown is rather large. Apparently, our computed T^{ij} obeys an approximate $1/\ln$ behavior within the range $|\hbar\Omega - 2\varepsilon(0)| < 0.01E_b$. One also sees that the T-matrix for $+-$ yields a better agreement with the Popov formula than that in the $++$ channel.

The results for the fit parameters A^{+-} and A^{++} with $\tilde{\gamma}_b = 10^{-3}$ as a function of m_e/m_h is shown in Figure 11. Without S, $A^{++}/2\pi\alpha(1-\alpha)$ deviates from 1.0 in the large m_e/m_h region. This is a result of the interaction Hamiltonian being strongly non-hermitian in this case. The value decreases to 1.0 as m_e/m_h decreases because the interaction Hamiltonian becomes more symmetric (see the discussion above). On the other hand, the results with S included is almost 1.0 because S recovers the hermiticity of the interaction Hamiltonian.

In the $+-$ channel, $A^{+-}/2\pi\alpha(1-\alpha)$ is close to 1.0 with and without S. The fact that it is close to 1.0 even without S, where the interaction Hamiltonian is non-hermitian, is due to a partial cancellation between the

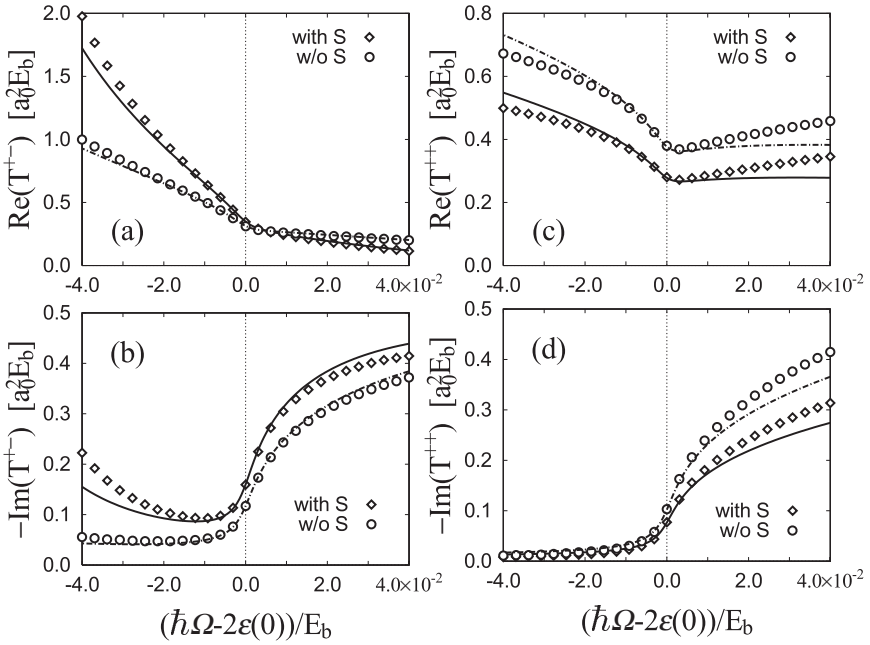

Fig. 10. Low energy behavior (*i.e.*, small deviations of the frequency argument from the two-exciton continuum edge) of the exciton-exciton (off-energy-shell) forward scattering amplitude at zero momentum in the counter-circularly (a, b) and co-circularly (c, d) polarization configuration for $\gamma_b/E_b = 3 \times 10^{-3}$. The full numerical results are shown as diamonds (circles) for calculations including (neglecting) the exciton overlap matrix S. The solid (dashed-dotted) lines show results obtained from fitting Popov's formula with (without) the exciton overlap matrix S.

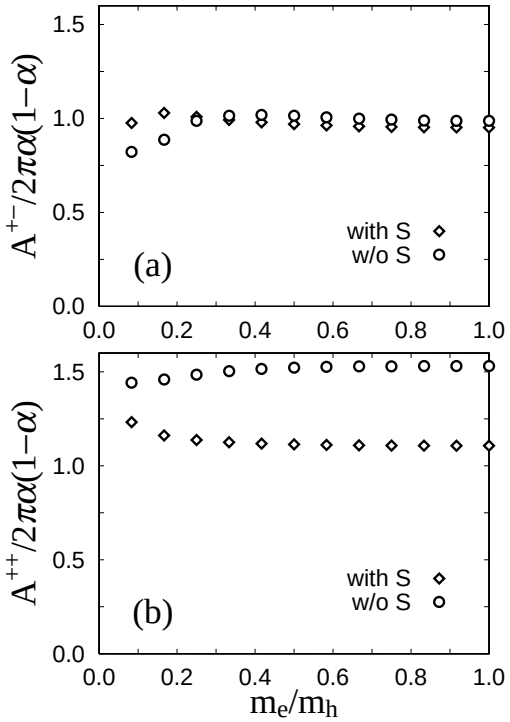

Fig. 11. The fit parameters A^{+-} (a) and A^{++} (b) *vs.* electron-hole mass ratio. The diamonds (circles) show the results obtained with (without) the exciton overlap matrix S. Here, $\alpha = m_{\rm h}/(m_{\rm e} + m_{\rm h})$.

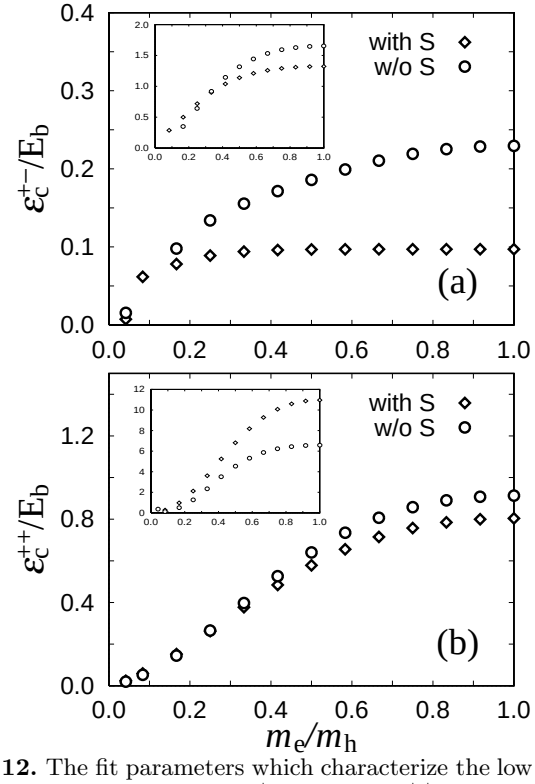

Fig. 12. The fit parameters which characterize the low energy behavior of the T-matrix, $\varepsilon_{\rm c}^{+-}$ (a) and $\varepsilon_{\rm c}^{++}$ (b) in units of the exciton binding energy E_b, calculated with (diamonds) and without (circles) the exciton overlap matrix S. Inset: The same data, but scaled by the biexciton binding energy, *i.e.*, $\varepsilon_c^{+-}/\varepsilon_{xx}$ and $\varepsilon_c^{++}/\varepsilon_{xx}$ (note that the ε_{xx} is a function of $m_{\rm e}/m_{\rm h}$).

$\mathcal{T}^+$ and $\mathcal{T}^-$ contributions (see Sect. 2.2 for the definition of T^{+-}).

In Figure 12 we show the characteristic energy scale ε_c^{ij}. These quantities increase monotonically as a function of electron-hole mass ratio. In other words, on the scale of the exciton binding energy the Popov formula is best fulfilled in semiconductors with equal electron and hole masses. As for the discrepancies one obtains in calculations with and without S, we show in the inset that scaling of ε_c^{ij} by the biexciton binding energy ε_{xx} modifies these discrepancies significantly (note that the biexciton binding energy also depends on the mass ratio).

4 Summary

We have presented a numerical analysis of the exciton-exciton interactions in a semiconductor quantum wells based on the dynamics-controlled-truncation (DCT) treatment of the quantum many-electron-hole system. Truncating the DCT equations to the heavy-hole 1s-exciton subspace (1s-approximation), we arrived at an effective exciton-exciton scattering theory, expressing the $\chi^{(3)}$ susceptibility in terms of an off-energy-shell exciton scattering (or T-) matrix.

We have discussed the validity of the 1s-approximation by evaluating exciton-exciton interaction matrix elements with states other than 1s; we have presented details of the exciton-exciton interaction matrix within the 1s-approximation, including the dependence on the electron-hole mass ratio and the issue of non-hermiticity; we have presented a comparison of the biexciton binding energies obtained within the 1s-approximation with literature values; we have studied the frequency dependence of the off-energy-shell excitonic T-matrix including its dependence on the exciton wave function overlap matrix S, its agreement (including numerical fits) at low energies with behaviors of generic T-matrices in 2-dimensional scattering theory, its dependence on the two-exciton dephasing rate γ_b (in particular the asymptotic value at zero-energy in the limit of vanishing γ_b).

Overall, we found that the exciton-exciton interaction matrix elements between 1s and higher states are small. This may be viewed as the basis for the validity of the 1s approximation, which may also be inferred from the fact that the obtained biexciton binding energy does not differ too much from established literature values. A detailed discussion contrasting our findings with publications which stress the role of higher (non-1s) exciton states has been given in Section 3.1. We also found that the excitonic T-matrix underlying 3rd-order optical susceptibilities exhibits the low energy asymptotic behavior of generic 2-dimensional two-body scattering amplitudes.

The inclusion of the excitonic wavefunction overlap matrix, S, essentially prevents the 1s-approximation from making the effective two-exciton Hamiltonian non-hermitian. On the other hand, we have found that, in the 1s approximation, S exhibits some problematic aspects that have led us to conclude that in quantitative applications its inclusion does not always improve the results. For one thing, the biexcitonic binding energy is less accurate in the calculations with S. The issue of whether to include S introduces an additional uncertainty that one should bear in mind when applying our theory in quantitative comparisons with experiments. The most reliable information is obtained in cases where one can draw physical conclusions whose validity are not too sensitive to this uncertainty. A nontrivial example of such a case has already been discussed in reference [44]. In view of the smallness of the Coulomb coupling between 1s and higher exciton states, we believe the magnitude and general functional form of the exact $\chi^{(3)}$ four-fermion 'T-matrix' around the two 1s-exciton continuum edge is quite reasonably represented by the 1s T-matrices (with or without S) presented here. Moreover, an important characteristic of the exact four fermion T-matrix, namely its vanishing at zero-frequency in the limit of vanishing γ_b [25], was found to be reproduced by the excitonic T matrix (independent of the inclusion of S). Detailed numerical accuracy can only be ascertained when the exact fermionic $\chi^{(3)}$ DCT theory is solved to the same level of numerical accuracy.

Our analysis should help to understand the physics of optical nonlinearities in the excitonic $\chi^{(3)}$-regime on the basis of standard scattering theory, while clarifying important differences between two-particle scattering with short-range potentials on the one hand and the physics of exciton-exciton scattering, which (even in the 1s-approximation) is a four-fermion problem, on the other hand.

This work is supported by grants from NSF (Division of Materials Research), JSOP, COEDIP (University of Arizona). We thank W. Schäfer for sending us part of his book (Ref. [38]) prior to publication and Y.P. Svirko and R. Shimano for useful discussions. One of us (R.T.) dedicates this paper to the memory of Hajime R. Takayama.

Appendix A: Angular momentum decomposition the interaction Hamiltonian

In this appendix, we show the details of the angular momentum decomposition (with the quantization axis normal to the plane of the quantum well) of the two-exciton Hamiltonian equation (18). As in the text, exciton-pair basis states in the center-of-mass frame are labeled by $(s_1, j_1, n, s_2, j_2, m, \mathbf{q})$, where n denotes the set of quantum numbers specifying the eigenstate of an exciton formed from an electron in the conduction band s_1 and a hole in the valence band j_1, the triplet m, s_2, j_2 specify the eigenstate of the other exciton, and $\mathbf{q}$ denotes the relative momentum between the two excitons. We will use polar coordinates for the momentum: $\mathbf{q} \equiv (q, \theta)$. We expand the column vectors and the matrix elements in this basis in

Fourier series in the angle coordinates:

$$b^{s_1 j_1 s_2 j_2 \lambda}_{nm}(\mathbf{q}) = \sum_{\mu} \mathrm{e}^{\mathrm{i}\mu\theta} b^{s_1 j_1 s_2 j_2 \lambda \mu}_{nm}(q) \tag{43}$$

$$\mathcal{N}^{j_1 j_2}_{nm,n'm'}(\mathbf{q},\mathbf{q}') = \sum_{\mu\mu'} \mathrm{e}^{\mathrm{i}\mu\theta} \mathcal{N}^{j_1 j_2 \mu\mu'}_{nm,n'm'}(q,q') \mathrm{e}^{-\mathrm{i}\mu'\theta'},$$
$$\mathcal{N} = W^{xx(\lambda)} \text{ or } S. \tag{44}$$

By the 2D rotational symmetry of our model exciton Hamiltonian, we can choose the exciton eigenstates to also be eigenstates of the exciton angular momentum l_z: $\phi^j_n(k,\theta_k) = f^j_n(k)\mathrm{e}^{\mathrm{i}\mu_n\theta_k}$ where μ_n is the l_z quantum number of state n and f^j_n is the radial eigenfunction. Then it can be shown, again by the rotational invariance of the unit operator and the Coulomb potential, the Fourier coefficients in equation (44) above are decoupled (diagonalized) into blocks labeled by the total angular momentum of the exciton-pair basis state $L_z = \mu + \mu_n + \mu_m$:

$$\mathcal{N}^{j_1 j_2 \mu\mu'}_{nm,n'm'}(q,q') = \delta_{\mu+\mu_n+\mu_m,\mu'+\mu_{n'}+\mu_{m'}} \frac{1}{2\pi} \times \int_0^{2\pi} \mathrm{d}\theta' \mathrm{e}^{\mathrm{i}\mu'\theta'} \mathcal{N}^{j_1 j_2}_{nm,n'm'}(q,0,q',\theta'), \tag{45}$$

where $\mathcal{N} = W^{xx(\lambda)}$ or S. Since the kinetic energy in equation (18) obviously has this property, the total (relative + internal orbital) angular momentum of the exciton pair L_z is conserved by the $(eehh)$ Hamiltonian, as expected from general considerations. The identity operator in the μ-basis is explicitly

$$I^{s_1 s_2 j_1 j_2 \mu\mu'}_{nm,n'm'}(q,q') = \delta_{nn'}\delta_{mm'}\delta_{\mu\mu'} 2\pi \frac{\delta(q-q')}{q}. \tag{46}$$

For spatially uniform exciting fields, it is a good approximation to assume the two excitons to be created in a state of zero L_z. If we further assume only the lowest exciton state $1s$ is excited, then the initial exciton pair has relative angular momentum $\mu = 0$. Subsequent scatterings will in general couple this initial state to states with other combinations of (μ_n, μ_m, μ) within the block satisfying $\mu_n + \mu_m + \mu = 0$. But if we further truncate the equations of motion (or, equivalently, the intermediate scattering states) to the $1s$ subspace, then the relative angular momentum μ is also conserved ($= 0$). Under these assumptions, the four-fermion Hamiltonian has been reduced to an effectively one-dimensional Hamiltonian, the nontrivial coordinate being the radial component of the relative momentum of the two $1s$ excitons.

Appendix B: Numerical construction of the exciton-exciton correlation kernel

In the equation of motion of the interband polarization equation (28), the correlation contribution is controlled by the 1s retarded exciton-exciton correlation kernel $\tilde{G}^{\lambda}(t-t')$. In this appendix, we lay out explicitly the numerical scheme for constructing this kernel *via* discretization (in the radial momentum coordinate). $\tilde{G}^{\lambda}(t-t')$ is defined by equation (22) restricted to the $1s$ subspace. Its non-trivial ingredient is the $1s$-restriction of equation (20): $\tilde{\mathcal{G}}^{\lambda}(\mathbf{q},\mathbf{q}',t-t') \equiv \frac{1}{\mathrm{i}\hbar}\theta(t-t')\left[\mathrm{e}^{-(\mathrm{i}/\hbar)(H^{xx(\lambda)}-\mathrm{i}\gamma_b I)(t-t')}\right](\mathbf{q},\mathbf{q}')$, which is the retarded Green's function of the Schrödinger equation under the Hamiltonian $H^{xx(\lambda)}$, *i.e.*,

$$\sum_{\mathbf{q}''}\left[\mathrm{i}\hbar\frac{\partial}{\partial t}\delta_{\mathbf{q}\mathbf{q}''} - H^{xx(\lambda)}(\mathbf{q},\mathbf{q}'') + \mathrm{i}\gamma_b\delta_{\mathbf{q}\mathbf{q}''}\right] \times\tilde{\mathcal{G}}^{\lambda}(\mathbf{q}'',\mathbf{q}',t-t') = \delta(t-t')\delta_{\mathbf{q}\mathbf{q}'} \tag{47}$$
$$\tilde{\mathcal{G}}^{\lambda}(\mathbf{q},\mathbf{q}',t-t') = 0, \quad t<t'.$$

We pass to the continuum limit of this equation, using the replacements: $\sum_{\mathbf{q}} \to \frac{1}{(2\pi)^2}\int \mathrm{d}q q \mathrm{d}\theta$, $\delta_{\mathbf{q}\mathbf{q}'} \to (2\pi)^2\delta(\theta-\theta')\frac{\delta(q-q')}{q}$. We then substitute $H^{xx(\lambda)}$ and $\tilde{\mathcal{G}}^{\lambda}$ by their double Fourier series (*cf.* Eq. (45)) and obtain the equation in angular momentum space. As noted above, $H^{xx(\lambda)}$ is block-diagonal in μ, leading to a one-dimensional equation for the Green's function of each value of μ. Only the $\mu = 0$ equation is considered, in which we will also suppress the index μ.

To evaluate the Green's function numerically, we discretize its equation on a grid in the radial momentum coordinate: $q_k = (k-1)\Delta q$, $k = 1,2,\cdots,N$, where Δq is the grid size and N the number of grid points. With $\delta(q_k - q_{k'}) \approx \frac{\delta_{kk'}}{\Delta q}$ and $\int \mathrm{d}q q \approx \sum_k \Delta q q_k$, the discretized equation for the $1s$, $\mu = 0$ Green's function takes the form

$$\sum_{k''}\left[\mathrm{i}\hbar\frac{\partial}{\partial t}\delta_{kk''} - H^{xx(\lambda)}_{kk''} + \mathrm{i}\gamma_b\delta_{kk''}\right] \times\tilde{\mathcal{G}}^{\lambda}_{kk''}(t-t') = \delta(t-t')\delta_{kk'} \tag{48}$$
$$\tilde{\mathcal{G}}^{\lambda}_{kk'}(t-t') = 0, \quad t<t'$$

where the discretized Hamiltonian is given by

$$H^{xx(\lambda)}_{kk'} = 2\varepsilon(q_k)\delta_{kk'} + \sum_{k''}(I-\lambda S)^{-1}_{kk''} W^{xx(\lambda)}_{k''k'} \tag{49}$$

with the various factors given in terms of the original functions in $\mathbf{q}$-space:

$$(1-\lambda S)_{kk'} = \delta_{kk'} - \lambda\frac{\Delta q q_{k'}}{2\pi}\int_0^{2\pi}\frac{\mathrm{d}\theta'}{2\pi} S(q_k,0,q_{k'},\theta') \tag{50}$$

$$W^{xx(\lambda)}_{kk'} = \frac{\Delta q q_{k'}}{2\pi}\int_0^{2\pi}\frac{\mathrm{d}\theta'}{2\pi} W^{xx(\lambda)}(q_k,0,q_{k'},\theta'). \tag{51}$$

The Green's function is constructed by an eigenvector expansion in this N-dimensional space. Let $\epsilon^{(\lambda)}_j$ and $\phi^{(\lambda)j}_k$, $j,k = 1,2,\cdots,N$ be the eigenvalues and the eigenvectors

respectively of $H^{xx(\lambda)}_{kk'}$. Then the discretized Green's function is given by

$$\tilde{\mathcal{G}}^{\lambda}_{kk''}(t-t') = \frac{1}{\mathrm{i}\hbar}\theta(t-t')\sum_{j=1}^{N} \mathrm{e}^{-\frac{\mathrm{i}}{\hbar}(\epsilon_j^{(\lambda)}-\mathrm{i}\gamma_b)(t-t')} U^{(\lambda)}_{kj}\left[U^{(\lambda)}\right]^{-1}_{jk'} \quad (52)$$

where the matrix $U^{(\lambda)}$ is assembled with the eigenvectors: $U^{(\lambda)}_{kj} = \phi^{(\lambda)j}_{k}$. Performing the same partial wave decomposition and discretization on the $1s$-restriction of equation (22), we obtain the following expression for the retarded two-exciton propagator:

$$\tilde{G}^{\lambda}(t-t') = \frac{1}{2}\sum_{k,k',k''=1}^{N}\left(\frac{\Delta q q_k}{2\pi}\right) W^{xx(\lambda)*} \times (q_k,0)\tilde{\mathcal{G}}^{\lambda}_{kk''}(t-t')(I-\lambda S)^{-1}_{k''k'} W^{xx(\lambda)}(q_{k'},0) \quad (53)$$

where $W^{xx(\lambda)}(q_k,0) = \int_0^{2\pi}\frac{\mathrm{d}\theta}{2\pi} W^{xx(\lambda)}(q_k,\theta,0,0)$.

References

1. M. Combescot, R. Combescot, Phys. Rev. Lett. **61**, 117 (1988).
2. M. Combescot, Phys. Rev. B **41**, 3517 (1990).
3. M. Kuwata-Gonokami, T. Saiki, in *Nonlinear Optics - Proceedings of the Fifth Toyota Conference on Nonlinear Optical Materials*, edited by S. Miyata (North-Holland, Amsterdam, 1992), pp. 329–334.
4. S. Bar-Ad, I. Bar-Joseph, Phys. Rev. Lett. **68**, 349 (1992).
5. V.M. Axt, A. Stahl, Z. Phys. B **93**, 205 (1994).
6. E.J. Mayer, G.O. Smith, V. Heuckeroth, J. Kuhl, K. Bott, A. Schulze, T. Meier, D. Bennhardt, S.W. Koch, P. Thomas, R. Hey, K. Ploog, Phys. Rev. B **50**, 14730 (1994).
7. E.J. Mayer, G.O. Smith, V. Heuckeroth, J. Kuhl, K. Bott, A. Schulze, T. Meier, S.W. Koch, P. Thomas, R. Hey, K. Ploog, Phys. Rev. B **51**, 10909 (1995).
8. W. Schäfer, D. Kim, J. Shah, T. Damen, J. Cunningham, K. Goossen, L. Pfeiffer, K. Köhler, Phys. Rev. B **53**, 16429 (1996).
9. A.E. Paul, J.A. Bolger, A.L. Smirl, J.G. Pellegrino, J. Opt. Soc. Am. B **13**, 1016 (1996).
10. P. Kner, S. Bar-Ad, M.V. Marquezini, D.S. Chemla, W. Schäfer, Phys. Rev. Lett. **78**, 1319 (1997).
11. V.M. Axt, K. Victor, T. Kuhn, Phys. Stat. Sol (b) **206**, 189 (1998).
12. G. Bartels, A. Stahl, Phys. Stat. Sol. (b) **206**, 325 (1998).
13. J.I. Inoue, T. Brandes, A. Shimizu, J. Phys. Soc. Jpn **67**, 3384 (1998).
14. J. Inoue, T. Brandes, A. Shimizu, Phys. Rev. B **61**, 2863 (2000).
15. H. Suzuura, Y. Svirko, M. Kuwata-Gonokami, Sol. Stat. Commun **108**, 289 (1998).
16. T. Östreich, K. Schönhammer, L. Sham, Phys. Rev. B **58**, 12920 (1998).
17. M. Kuwata-Gonokami, S. Inoue, H. Suzuura, M. Shirane, R. Shimano, T. Someya, H. Sakaki, Phys. Rev. Lett. **79**, 1341 (1997).
18. M. Shirane, C. Ramkumar, Y.P. Svirko, H. Suzuura, S. Inoue, R. Shimano, T. Someya, H. Sakaki, M. Kuwata-Gonokami, Phys. Rev. B **58**, 7978 (1998).
19. G. Bartels, A. Stahl, V. Axt, B. Haase, U. Neukrich, J. Gutowski, Phys. Rev. Lett. **81**, 5880 (1998).
20. H. Fan, H. Wang, H.Q. Hou, B.E. Hammons, Phys. Rev. B **57**, R9451 (1998).
21. T. Aoki, G. Mohs, M. Kuwata-Gonokami, Phys. Rev. Lett. **82**, 3108 (1999).
22. H.P. Wagner, A. Schätz, W. Langbein, J.M. Hvam, A.L. Smirl, Phy. Rev. B **60**, 4454 (1999).
23. Y.P. Svirko, M. Shirane, H. Suzuura, M. Kuwata-Gonokami, J. Phys. Soc. Jpn **68**, 647 (1999).
24. P. Borri, W. Langbein, J.M. Hvam, F. Martelli, Phys. Rev. B **60**, 4505 (1999).
25. T. Östreich, L.J. Sham, Phys. Rev. Lett. **83**, 3510 (1999).
26. C. Sieh, T. Meier, F. Jahnke, A. Knorr, S. Koch, P. Brick, M. Hübner, C. Ell, J. Prineas, G. Khitrova, H. Gibbs, Phys. Rev. Lett. **82**, 3112 (1999).
27. J. Shah, *Ultrafast Spectroscopy of Semiconductors and Semiconductor Nanostructures*, Vol. 115 of *Springer Series in Solid-State Sciences* (Springer, Berlin, 1996).
28. V.M. Axt, A. Stahl, Z. Phys. B **93**, 195 (1994).
29. U. Neukirch, S.R. Bolton, N.A. Fromer, L.J. Sham, D.S. Chemla, Phys. Rev. Lett. **84**, 2215 (2000).
30. V.M. Axt, B. Haase, U. Neukirch, Phys. Rev. Lett. **86**, 4620 (2001).
31. L.I. Schiff, *Quantum Mechanics* (McGraw-Hill, New York, 1968).
32. R.G. Newton, *Scattering Theory of Waves and Particles*, 2nd edn. (Springer, New York, 1982).
33. V.N. Popov, *Functional Integrals in Quantum Field Theory and Statistical Physics* (Reidel, Dordrecht, 1983).
34. M. Schick, Phys. Rev. A **3**, (1971) 1067, for example, equation (4) in this reference shows how to obtain the chemical potential of an interacting 2D Bose gas from the T-matrix.
35. R. Machleidt, Adv. Nucl. Phys. **19**, 189 (1989).
36. P. Kner, S. Bar-Ad, M.V. Marquezini, D.S. Chemla, R. Lövenich, W. Schäfer, Phys. Rev. B **40**, 4731 (1999).
37. R. Lövenich, thesis (John von Neumann- Institut für Computing, Jülich, 2000).
38. W. Schäfer, M. Wegener, *Semiconductor optics and transport - from fundamentals to current topics* (Springer, Berlin, 2002), to be published.
39. H. Haug, S. Schmitt-Rink, Prog. Quantum Electron. **9**, 3 (1984).
40. A. Ivanov, H. Haug, Phys. Rev. B **48**, 1490 (1993).
41. C. Ciuti, V. Savona, C. Piermarocchi, A. Quattropani, P. Schwendimann, Phys. Rev. B **58**, 7926 (1998).
42. D.A. Kleinman, Phys. Rev. B **28**, 871 (1983).
43. Y. Suzuki, K. Varga, *A stochastic variational approach to quantum-mechanical few-body problems* (Springer, Berlin, 1998).
44. N. Kwong, R. Takayama, I. Rumyantsev, M. Kuwata-Gonokami, R. Binder, Phys. Rev. B **64**, 45316 (2001).
45. N. Kwong, R. Takayama, I. Rumyantsev, M. Kuwata-Gonokami, R. Binder, Phys. Rev. Lett. **87**, 27402 (2001).